Pergamon

Bioorganic & Medicinal Chemistry, Vol. 5, No. 2, pp 335–352, 1997

PII: S0968-0896(96)00252-0
0968-0896/97 $17.00 + 0.00

Conformational Analysis of Glutamic Acid Analogues as Probes of Glutamate Receptors using Molecular Modelling and NMR Methods. Comparison with Specific Agonists

Nathalie Todeschi,[a] Josyane Gharbi-Benarous,[a,b] Francine Acher,[a] Valery Larue,[a] Jean-Philippe Pin,[c] Joël Bockaert,[c] Robert Azerad[a] and Jean-Pierre Girault[a,*]

[a]*Université René Descartes-Paris V, Laboratoire de Chimie et Biochimie Pharmacologique et Toxicologique (URA 400 CNRS), 45 rue des Saints-Pères, 75270 Paris Cedex 06, France*

[b]*Université Denis Diderot-Paris VII, UFR Chimie, 2 Place Jussieu, F-75251 Paris Cedex 05, France*

[c]*Centre CNRS-INSERM de Pharmacologie-Endocrinologie, UPR 9023 Mécanisme Moléculaires des Communications Cellulaires, rue de la Cardonille, 34094 Montpellier Cedex 5, France*

Abstract—The activity of five glutamic acid analogues substituted in position 3 or 4 by a methyl (**3T**, **3E**, **4T**, and **4E**) or a methylene group (**4M**) has been examined at one cloned Glu receptor subtype, $mGluR_1$. These analogues interact with glutamate receptors of the central nervous system, especially the ligand **4T** [(2*S*,4*S*)-4-methylglutamic acid] at the metabotropic glutamate receptor $mGluR_1$. It was observed that only the **4T** isomer is as potent an agonist as glutamic acid, whereas other isomers are less active. Furthermore, **4E** [(2*S*,4*R*)-4-methylglutamic acid] exhibited an exceptional selectivity for the KA ionotropic receptor subtype while **4M** [(2*S*)-4-methyleneglutamic acid] was active at the NMDA receptors. These molecules represent suitable tools among a population of similar glutamate analogues for a classical structure–function relationship study. We have undertaken a conformational analysis by ^1H and ^{13}C NMR spectroscopy and molecular modelling of these molecules. Hetero- and homonuclear coupling constants were measured in order to assign the diastereotopic methylene protons at C(3) or C(4), and used for comparison in molecular dynamics (MD) simulations. The hydrogen-bonding possibility, steric effects or electrostatic interactions may be a considerable influence in stabilizing a conformational population in D_2O solution. The conformations may be grouped by the two backbone torsion angles, χ_1 [α-CO_2^-–C(2)–C(3)–C(4)] and χ_2 [$^+NC(2)$–C(3)–C(4)–γCO_2^-] and by the two characteristic distances between the potentially active functional groups, αN^+—γCO_2^- (d_1) and αCO_2^-—γCO_2^- (d_2). The conformational preferences in solution of **4T**, **4E** and (**3T**, **3E**, **4M**) are discussed in the light of the physical features known for a specific metabotropic agonist (ACPD) and specific ionotropic agonists (KA) and (NMDA), respectively.

Introduction

Glutamate is the neurotransmitter at most fast excitatory synapses in the mammalian central nervous system (CNS).[1,2] It plays an important role in synaptic plasticity phenomena involved in brain development, learning. and memory.[3] Glutamate is also the main endogenous neurotoxin, being responsible for neuronal death observed after ischemy, hypoxy, or hypoglycemy.[4] Glutamate is therefore assumed to be involved in some neurological disorders such as Parkinson's and Alzheimer's diseases and Huntington's chorea.

Glutamate activates two types of receptors, the ionotropic and the metabotropic.[5–7] The ionotropic receptors are multimeric glutamate-gated channels permeable to cations and responsible for fast depolarization.[5,6] Three subtypes have been characterized based on their channel properties, pharmacology, and subunit composition. They are termed NMDA (*N*-methyl-D-aspartate), AMPA (α-amino-3-hydroxy-5-methylisoxazole-4-propionate), and KA (kainate) receptors. The metabotropic glutamate receptors (mGluRs) have been characterized more recently and correspond to receptors coupled to G-proteins and modulating the activity of ionic channels or enzymes producing second messengers.[7,8] They are involved in the modulation of the fast synaptic transmission, and their physiological role appears to be more important than previously expected. Interestingly, these receptors are involved in glutamate-induced synaptic plasticity,[9–11] and in spacial[9,10] and olfactory[12] memory. Today, eight mGluRs have been characterized and classified into three groups based on their sequence homology, transduction mechanism, and pharmacology.[8] Group-I is composed of $mGluR_1$ and $mGluR_5$, which are coupled to phospholipase C and are activated by (1*S*,3*R*)-ACPD and quisqualate. $mGluR_2$ and $mGluR_3$, which are activated by (1*S*,3*R*)-ACPD, are negatively coupled to adenylyl cyclase and constitute group-II. Group-III is composed by all other mGluRs, also negatively coupled to adenylyl cyclase but selectively activated by L-AP4.

The recent characterization of the agonist binding site of glutamate receptors revealed the main originality of all glutamate receptors compared to all other receptors characterized so far.[13,14] In glutamate receptors, the agonist recognition domain is homologous to amino acid binding proteins found in the periplasmic space of

bacteria. These proteins are constituted by two lobes with a hinge region where the agonist binds. Upon binding of the ligand, the two lobes close like a clamshell. Based on the homology with leucine, isoleucine, valine binding protein (LIVPB), a three-dimensional model has been proposed for the agonist recognition domain of $mGluR_1$. This model has been confirmed by point mutation affecting the glutamate affinity.[13]

In order to examine the conformational requirements of L-Glu for stimulating each Glu receptors subtype,[15] we must determine both the biological activity at specific Glu receptors and the conformation of a series of glutamic acid analogues.

In this study, the activity of five glutamic acid derivatives substituted in position β- or 3 and γ- or 4 by a methyl (**3T**, **3E**, **4T**, **4E**) or a methylene (**4M**) group (Fig. 1a) is examined with respect to one Glu receptor subtype, $mGluR_1$. This receptor has been chosen because its agonist recognition site has been the subject of intense research and is therefore better characterized.[13] Literature results on KA and NMDA receptors are discussed; thereafter, a conformational analysis by ^1H and ^{13}C NMR spectroscopy and molecular modelling of these molecules is presented.

We previously analysed by NMR spectroscopy and molecular dynamics (MD) the conformation of cyclic analogues of glutamic acid containing a cyclohexane and a cyclopentane ring,[16,17] whose biological activities had been described.

The methylated molecules are more flexible than the cyclic analogues.[16,17] They can thus adopt conformations that may help them to be recognized by the receptor. They allow a more differentiated exploration of the geometry of the binding site according to the observed biological activities. The practical methodologies employ molecular dynamics to generate conformations and include experimental analysis to determine the 3-D stucture from NMR data. The modelling procedure used to generate the approximate ratios of low-energy conformers will also specify the structures representative of very hindered intermediates.

The receptor may be an acceptor or donor of protons. Hence, it was interesting to examine the conformational changes induced by the electrostatic field generated by the different polarities of these molecules. We have extended the NMR and the MD studies in water at different pH values, so as not to neglect protonation effects which will induce particular conformations.

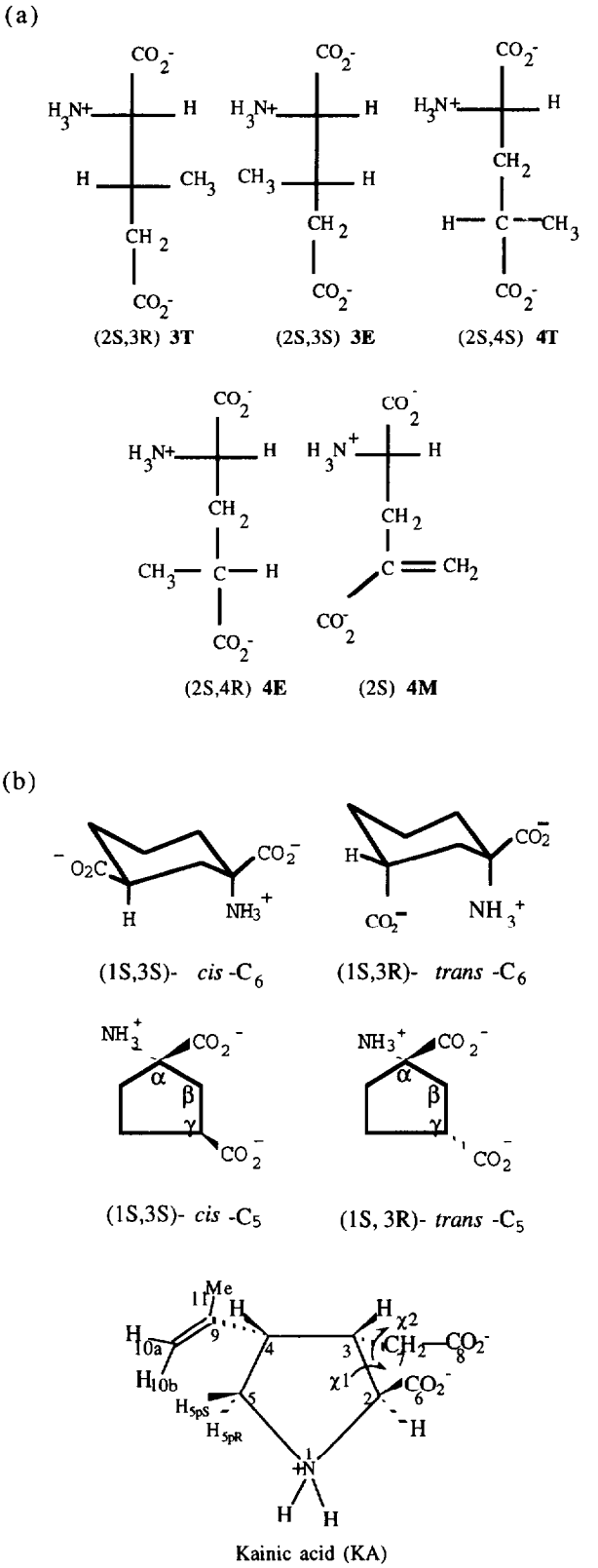

Figure 1. (a) Structures of the five amino acid analogues studied in aqueous solution at pH 7: 3-methyl glutamic acid **3T**, **3E**, 4-methyl glutamic acid **4T**, **4E** and 4-methylene glutamic acid **4M** (isomers α-S represented). (b) Structures of kainic acid and *cis*-C6, *trans*-C6, *cis*-C5, *trans*-C5 analogues of the glutamic acid in aqueous solution at pH 7, (isomers α-S represented). (The definition of *cis* and *trans* is relative to the arrangement of the carboxyl function. *cis*-C6 or -C5 is an equimolecular mixture of 1*S*,3*S* and 1*R*,3*R* and *trans*-C6 or -C5 an equimolecular mixture of 1*S*,3*R* and 1*R*,3*S*).

Results and Discussion

Biological activity

The cyclic glutamic acid analogues, the *cis*- and *trans*-C6 and -C5 (Fig. 1b) have already been tested for some biological properties in a comparison with

glutamic acid.[18] In non-NMDA receptors, the *cis*-C6 isomer has been shown to be an effective agonist and the *trans*-isomer to be much less active. Among the ACPD analogues, (1*R*,3*R*)-*cis*- and (1*S*,3*R*)-*trans*-C5, only the *cis* isomer is an agonist of the NMDA receptor. The (1*S*,3*R*)-*trans*-ACPD activates both metabotropic subtypes group-I ($mGluR_1$, $mGluR_5$) and group-II ($mGluR_2$, $mGluR_3$). It also has some activity at high concentration with the other four $mGluR_{4-8}$ but has no activity on ionotropic receptors.

The five substituted derivatives[19] (**3T**, **3E** and **4T**, **4E**, **4M**) (Fig. 1a) have been tested on the '$mGluR_{1a}$' receptor expressed in *Xenopus* oocytes and only one isomer, the [(2*S*,4*S*)-4-methylglutamic acid] **4T** exhibited an activity similar to glutamate, thus suggesting the existence of a particular conformational preference. The other isomers are less active.[20] This '$mGluR_{1a}$' receptor that is activated by (1*S*,3*R*)-*trans*-ACPD and more potently by the **4T** isomer, consists of one subunit and is coupled to phospholipase C.

Moreover, some of these analogues have been tested at the ionotropic receptor. The introduction of a methyl group at the 4-position, resulting in conformational changes of the molecule, enhances the selectivity at the KA receptor.[21] The (2*S*,4*R*)-4-methylglutamic acid **4E** has been identified as having exceptional selectivity for KA receptor subtype with an IC_{50} for inhibition of [^{3}H]KA binding comparable to kainic acid itself.[21]

Some neurobiological tests have been carried out on the 4-methylene-L-glutamate (**4M**) and the preliminary accounts of electrophysiological experiments in the new born rat spinal cord have shown (as is observed for the (1*R*,3*R*)-*cis*-ACPD) that the depolarizing activity of this compound is 10 times more potent than that of L-glutamate. The depolarization of 4-methylene-L-glutamate (**4M**) is due to the activation of NMDA receptors among three representative ionotropic glutamate receptors (NMDA, kainate, and AMPA receptors).[22]

These molecules represent a suitable tool among a number of similar glutamate analogues for a classical structure–function relationship study. The comparison between these five analogues with kainic acid,[23] (1*R*,3*R*)-*cis*-ACPD and (1*S*,3*R*)-*trans*-ACPD compounds will prove to be useful in sorting out some structural differences.

Conformational analysis

It is difficult to study the conformation of the linear methylated analogues[24] (Fig. 1a) because in these molecules there is a high degree of freedom around the C(2)–C(3) torsion angle χ_1 and the C(3)–C(4) torsion angle χ_2. The C(2)–C(3)–C(4) system with two C—C single bonds allows the possibility of *trans* and *gauche* forms and there are a total of $3 \times 3 = 9$ rotamers, all of which are distinct. The 'A' (*t*) orientation characterizes the χ_1 angle [α-CO_2^-–C(2)–C(3)–C(4)] (170°) while the 'B' (g^+) and the 'C' (g^-) characterize the χ_1 angle (+60°) and (−60°), respectively. In the same order, the letters 'a, b, and c' characterize conformations for the rotamers about the χ_2 angle [N^+C(2)–C(3)–C(4)–γCO_2^-] (170°), (+60°), and (−60°), respectively. We obtain nine Aa, Ab, Ac, Ba ... (or six Aβ, Aγ... for **4M**) staggered conformations resulting from the combination of the three rotamers 'A, B, and C' relative to the χ_1 torsion angle [C(2)-C(3)] with the three rotamers 'a, b, and c (or β, γ for **4M**)' relative to the χ_2 torsion angle [C(3)–C(4)] (Fig. 2).

The conformations will be grouped into four conformational families I to IV, characterized by the two distances between the potentially active functional groups, αN^+—γCO_2^- (d_1) and αCO_2^-—γCO_2^- (d_2). Two families will be characterized by a d_1 distance shorter than d_2: I ($d_1 \ll d_2$) and II ($d_1 < d_2$). Conversely, two other families will be characterized by a d_2 distance shorter than d_1: III ($d_2 < d_1$) and IV ($d_2 \ll d_1$). Since this classification, the privileged conformations of the different active analogues will be used to establish a correlation between their structures and their corresponding activities at metabotropic or ionotropic receptors.

These derivatives exist as highly charged molecules. Thus, in order not to neglect the protonation effect, this study is extended to different pH values to use NMR and MD searching for the particular induced conformations. At isoelectric pH (pH_i 3) the γ-carboxylate group is protonated and can provide a distal carboxylic acid that possesses a potential proton donor hydroxyl group; at the opposite end of the scale, at pH 10, the amino group carries no formal charge. The nomenclature used in this paper is defined as following: the first number indicates the position of the methyl or methylene (at carbon **3** or **4**), the second one the predominant form in the pH zone considered (isoelectric zone **1**, neutral zone **2**, and alkaline zone **3**), the letter **E** or **T** the relative configuration of the methyl and **M** the methylene substituent.

NMR spectroscopy

The assignments are made for the five compounds in D_2O solution at three pH values (3, 7, and 10) using 1-D, ^{1}H and ^{13}C (^{1}H decoupled and DEPT-135) spectra and heteronuclear (F1 decoupled) shift correlations. The ^{1}H NMR spectrum at 500.13 MHz exhibits four spin systems and in all cases, the starting point is the signal of the H(2) proton (because of the adjacent α-CO_2^- and α-NH_3^+ groups). In the ^{13}C NMR spectrum (125.76 MHz), one-dimensional selective INEPT experiment[25b] based on a selective excitation of the H(2) proton, it is useful to differentiate both α- and γ-carboxylate groups. However, less ambiguous is a correlation in the HMBC, in this case the correlation from H(2) to α-CO_2^-. The different isolated carboxylate groups of **4M** are only identified in the HMBC by their correlations via two- [H(2) to α-CO_2^-] and three-bond [H(6) to γ-CO_2^-] couplings. The complete assignment of the ^{1}H (500.13 MHz) and ^{13}C NMR (125.76 MHz)

signals of the five isomers is achieved at different pH values.

For the **3E**, **3T**, **4E** and **4M** isomers, the coupling constants are deduced from 1-D spectra at 500 MHz and are confirmed by spectral simulation with 'NMR II' program (Table 1). For the **4T** isomer, the spin system is complex as the protons constitute a highly coupled system, H(3a), H(3b), H(4). The *J*- and δ-values are thus calculated from 1-D spectra at 500 MHz after irradiation of the H(2) proton and confirmed by NMR simulation (NMR II program).

Besides the conformational analysis (rotamer populations), coupling constants are used to determine the assignment of the individual diastereotopic methylene protons, which is particularly difficult.[26] The homonuclear coupling constants are not sufficient to allow unambiguous assignments. Hence, it was necessary to define the $^3J_{(C,H)}$ coupling constants of both diastereotopic protons and use these values in conjunction with the $^3J_{(H,H)}$ to define the conformation of the C(2)–C(3)–C(4) fragment (Table 1). The ^{13}C–^1H coupling constants are 'out of phase' with the ^1H–^1H coupling constants so that in rotamer **4T A**, for example, $H(3)_{proR}$ and $H(3)_{proS}$ are both *gauche* to the carboxyl carbon C(1), but are *gauche* and *trans*, respectively, to the proton H(2); while in rotamer **b** $H(3)_{proR}$ is *gauche* to the carboxyl carbon C(5), but *trans* to the proton H(4) and conversely for $H(3)_{proS}$ (Fig. 2). One method for the quantitative determination of heteronuclear coupling constants usually fulfils these demands: the 2-D *J*δ selective INEPT[27] using polarization transfer from ^1H to ^{13}C. The homonuclear and heteronuclear three-bond coupling constants necessary for the assignments of the diastereotopic protons at C(3) and C(4) are listed in Table 1.

Using the assignments of the diastereotopic CH_2 protons, the preferred conformation of the C(2)–C(3) and C(3)–C(4) torsion can be calculated from (i) the values of vicinal $^3J_{HH}$ and $^3J_{CH}$ experimental coupling constants in D_2O solution, reported in Table 1 and (ii) the corresponding coupling constants calculated by a Karplus-type equation[26,28] from all the theoretical structures. The Karplus-type equations with different coefficients in the homonuclear case,[26a] A = 9.5, B = −1.3, and C = 1.6 and in the heteronuclear case,[28b] A = 5.7, B = −0.6, and C = 0.5, give approximately $J_g = 3.3$ Hz and $J_t = 12.4$ Hz for $^3J_{HH}$, and $J_g = 1.8$ Hz and $J_t = 6.5$ Hz for $^3J_{HC}$.

The experimental values of $^3J_{^1H\text{-}^1H}$ and $^3J_{^{13}C\text{-}^1H}$ are averaged. Thus, it is possible to interpret these values

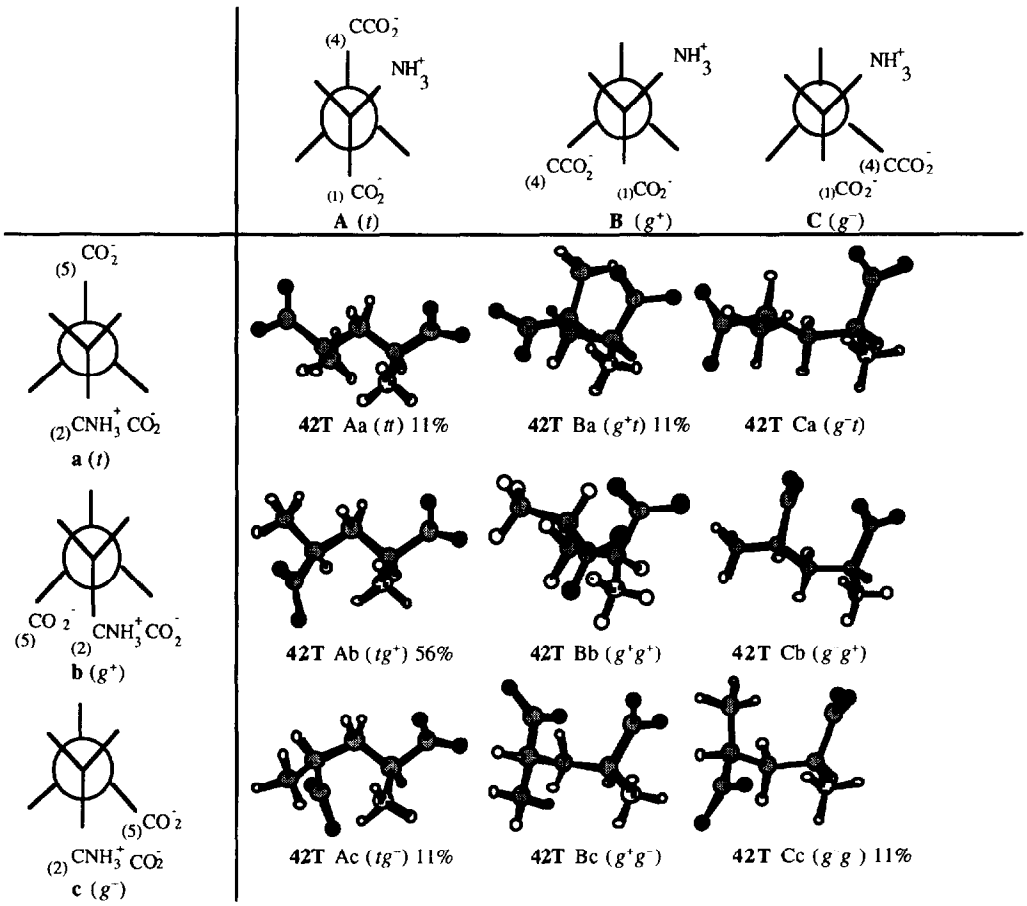

Figure 2. Newmann projections for the three rotamers 'A, B, and C' relative to the torsion angle χ_1 (C2–C3) and 'a, b, and c' relative to the χ_2 one (C3–C4) (*t* = *anti* and *g* = *gauche*). The nine conformations (Aa; Ab; Ac; Ba; Bb; Bc; Ca; Cb; Cc) of one analogue (**4T**), generated at pH 7 and the frequency of each conformation obtained with MD protocol in solvation box.

as a population of the three rotamers[25c] 'A, B, and C' (dihedral angle χ_1) and the three ones 'a, b, and c' (dihedral angle χ_2).

$$^3J_{2,3a} \text{ or } ^3J_{2,3b\ exp} = P_A J_g + P_B J_t + P_C J_g \quad (1)$$

$$^3J_{C(4)H(2)\ exp} = P_A J_g + P_B J_t + P_C J_g \quad (2)$$

$$P_A + P_B + P_C = 1. \quad (3)$$

J_g and J_t indicate the $^3J_{2,3}$ coupling constant for the H(2) and H(3) protons in the *gauche* and *trans* configuration, respectively.

At neutral pH, the study was made at different temperatures (280, 290, 300 and 310 K) to analyze the evolution of the different populations in the conformational equilibrium, but the observed coupling constants do not change appreciably as the temperature increases.

Thus, the experimentally determined coupling constants $^3J_{^1H,^1H}$ and $^3J_{^{13}C,^1H}$ presented in Table 1 allow us to determine with tolerable precision the mole fractions for each rotamer P_A, P_B and P_C or P_a, P_b, and P_c; it appears that rotamer populations accurate to $\pm 10\%$ can still be obtained. Considering the rotamer distribution for the glutamic acid analogues **3E**, **3T**, **4E**, **4T**, and **4M**, the major species in aqueous solution are A (t) and c (g^-) for **3T**, C (g^-) and b (g^+) for **3E**, A (t) and b (g^+) for **4T**, A (t) and c (g^-) for **4E** and B (g^+) and γ (g) for **4M**.

These results emphasize the specificity of the influence of methyl (or methylene) position. Furthermore, these data will be confirmed in the molecular modelling work.

At pH 3 (Table 1), when the 3-carboxy group and the 1-amino group are protonated, the couplings corresponding to the first torsion angle χ_1 and the second torsion angle χ_2 show that an equilibrium still occurs for the five analogues, but not with the same proportions. The protonation effect may be an influence in stabilizing new conformations of rotamers. The 'B and b' conformers (g^+) are very likely stabilized by an electrostatic interaction (such as a hydrogen bond) between the 1-carboxylate and the 3-carboxy groups.

At alkaline pH (Table 1), the preferred conformations are the sterically favoured one 'A' (for χ_1) and 'a' (for χ_2) and the most populated rotamers in solution are A (t) and a (t) for **33T** and **43T**, C (g) and a (t) for **33E**, A (t) and c (g^-) for **43E**, and A (t) and γ (g^-) for **43M**.

Table 1. Homonuclear ($^1H,^1H$) and heteronuclear ($^{13}C,^1H$) coupling constants in D_2O (Hz, error 0.5 Hz) used in the conformational analysis of the five isomers (**3T**, **3E**, **4T**, **4E**, and **4M**) and for the assignment of the diastereotopic methylene protons at C(3) or C(4). The first number indicates the position of the methyl or methylene (at carbon **3** or **4**), the second one the predominant form in the pH zone considered (isoelectric zone **1**, neutral zone **2** and alkaline zone **3**), the letter **E** or **T** the relative configuration of the methyl and **M** the methylene substituent

	^3J (Hz)																
	3T			**3E**				**4T**			**4E**				**4M**		
	31T	**32T**	**33T**	**31E**	**32E**	**33E**		**41T**	**42T**	**43T**	**41E**	**42E**	**43E**		**41M**	**42M**	**43M**
2,3	2.4	3.5	3.2	3.5	4.0	5.0	2,3a	7.4	8.9	9.4	4.7	4.5	5.0	2,3a	3.8	3.7	3.7
3,4a	5.7	5.2	5.0	5.1	4.6	3.4	2,3b	6.4	4.8	6.0	7.9	8.2	8.2	2,3b	8.1	8.3	8.3
3,4b	7.4	7.8	9.6	8.0	8.3	11.4	3a,4	8.1	7.3	5.8	8.9	8.8	8.2	2-H,4-C		4.8	
4a-H,2-C		3.9			4.3		3b,4	6.5	7.3	10.0	5.1	5.2	6.5	3a-H,1-C		4.4	
4a-H,3Me-C		5.2			4.6		4-H,2-C		2.7			3.2		3a-H,5-C		5.7	
4b-H,2-C		3.0			2.7		2-H,4-C		3.3			4.1		3a-H,6-C		3.3	
4b-H,4Me-C		5.0			4.6		3a-H,1-C		2.8			3.9		3b-H,1-C		1.5	
2-H,4-C		3.3			4.7		3a-H,5-C		2.0			3.5		3b-H,5-C		5.2	
2-H,3Me-C		5.0			3.6		3a-H,4Me-C		4.2			3.4		3b-H,6-C			
3-H,5-C		—			<2		3b-H,1-C		2.6			2.5					
3-H,1-C		—			3.2		3b-H,5-C		5.0			6.0					
							3b-H,4Me-C		3.7			3.5					
Assignment							Assignment							Assignment			
4a-H		*ProR*			*ProS*		3a-H		*ProR*			*ProS*		3a-H		*ProR*	
4b-H		*ProS*			*ProR*		3b-H		*ProS*			*ProR*		3b-H		*ProS*	
	Populations of rotamers[a] about χ_1 and χ_2																
A	72	72	70	6	15	14		49	65	70	54	55	58		10	10	60
B	1	5	5	32	30	28		38	20	25	19	20	22		60	60	10
C	27	23	25	62	55	58		13	15	5	27	25	20		30	30	30
a	30	27	73	24	20	93		30	35	75	22	20	30				
b	25	23	4	55	55	4		60	50	20	34	25	30				
c	45	50	22	21	25	2		10	15	5	44	55	40				
β															35	25	35
γ															65	75	65

[a]The major populations of rotamers about χ_1 and χ_2 are underlined.

A variety of possibilities enable the conformational populations to be assessed from rotamers in NMR solution. Thus, it is very important to compare the NMR results to those obtained from molecular modelling in order to identify the corresponding solution conformations at different pH values.

Molecular modelling

Molecular mechanics

The different conformations of the **3T**, **3E**, **4T**, **4E**, and **4M** isomers were minimized by molecular mechanics. A widely used method to mimic the solvent screening effect is to use a distance-dependent relative dielectric constant $\varepsilon = r$, leading to an r^2 dependence of the coulombic energy.[29] In previous studies, the relative dielectric constant was adjusted to a value $\varepsilon = 5$ corresponding to the interactions in aqueous solution.[15] Using the Boltzmann distribution, the relative population of each conformer is given by the following expression:

$$P_i = \exp(-E_i/kT)/\Sigma\exp(-E_i/kT) \quad (4)$$

Upon direct minimization with $\varepsilon = 5$, an electrostatic attraction between the α-NH_3^+ and the γ-CO_2^- groups leads to the lowest energy structure Ab, in the case of the five isomers, but this is not entirely consistent with the NMR results. So, we either reduce the electrostatic contribution by using $\varepsilon = 78$ or we performe minimization in a solvent box (Fig. 3) with the introduction of explicit water molecules in order to reduce the electrostatic contribution. This last protocol is not of practical use, as the energies of the corresponding minimized molecules and thus their relative populations are very difficult to evaluate (the energies obtained are those of 'molecule + 48 H_2O' systems).

For these charged, flexible methylated molecules, it is obvious that other methods may have to be used in a MD study to obtain a more reasonable statistical participation of every structure. We performed MD runs for the nine conformations of each compound. The results are summarized in Figures 4 and 5 and in Table 2.

Molecular dynamics

The MD simulations were carried out using the DISCOVER program of BIOSYM molecular modelling software on a Silicon Graphics workstation.

First, for an exploration of the conformational space, after an equilibration period of 4 ps, the dynamics are

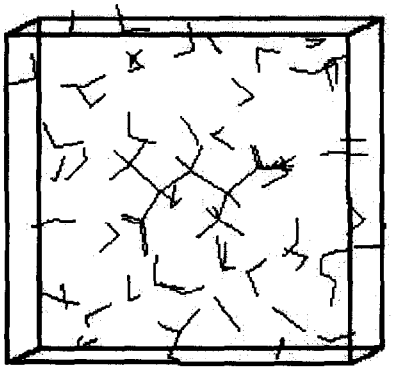

Figure 3. Solvation box containing the **4T** molecule and several water molecules (**4T** + 48 H_2O) to mimic the solvent effect with explicit modelling of water in molecular dynamics protocol.

Table 2. Results (%) of the MD simulations for **3T**, **3E**, **4T**, **4E**, and **4M** at different pH values. Percentage of each conformation generated starting from the nine (or six) conformations of each isomer

	3T			**3E**			**4T**			**4E**				**4M**		
	31T pH 3	**32T** pH 7	**33T** pH 10	**31E** pH 3	**32E** pH 7	**33E** pH 10	**41T** pH 3	**42T** pH 7	**43T** pH 10	**41E** pH 3	**42E** pH 7	**43E** pH 10		**41M** pH 3	**42M** pH 7	**43M** pH 10
Aa	13	11	58	11	0	45	11	11	38	10	0	10	**Aβ**	4	16	10
Ab	11	34	3	0	11	0	13	56	12	20	34	7	**Aγ**	27	5	50
Ac	20	22	25	11	15	16	17	11	19	20	22	23	**Bβ**	20	0	20
Ba	20	11	0	0	0	15	0	11	10	10	22	23	**Bγ**	32	60	0
Bb	11	0	0	23	30	0	31	0	6	0	0	15	**Cβ**	13	11	0
Bc	4	0	0	11	0	0	6	0	0	10	0	0	**Cγ**	4	8	20
Ca	5	0	14	11	0	24	6	0	15	0	0	7				
Cb	0	0	0	22	13	0	5	0	0	10	0	8				
Cc	18	22	0	11	31	0	11	11	0	20	22	7				
	Populations of rotamers[a] about χ_1 and χ_2															
A	44	67	86	22	26	61	41	78	69	50	56	40	**A**	31	21	60
B	35	11	0	34	30	15	37	11	16	20	22	38	**B**	52	60	20
C	23	22	14	44	44	24	22	11	15	30	22	22	**C**	17	19	20
a	38	22	72	22	0	84	17	22	63	20	22	40	**β**	37	27	30
b	22	34	3	45	54	0	49	56	18	30	34	30	**γ**	63	73	70
c	42	44	25	33	46	16	34	22	19	50	44	30				

[a]An ensemble of nine separate trajectories of 100 ps starting from nine separate staggered conformations was calculated for a reliable statistical convergence and we have reported populations of rotamers (%) about χ_1 and χ_2 from the percentage of each conformation generated with the different protocols (for each isomer 900 or 1800 structures were examined).

run at 300 K with periodic jumps to 600 K as the large amount of kinetic energy present at high temperature allows high potential energy barriers to be crossed. For the five analogues, a 50 ps MD experiment is run[30] starting from the nine possible conformations of each isomers, at three pH values. Then, the stability of the different conformers was tested by a 200 ps dynamics protocol at 300 K. The experiments are first carried out with the value of the relative dielectric constant $\varepsilon = 5$,

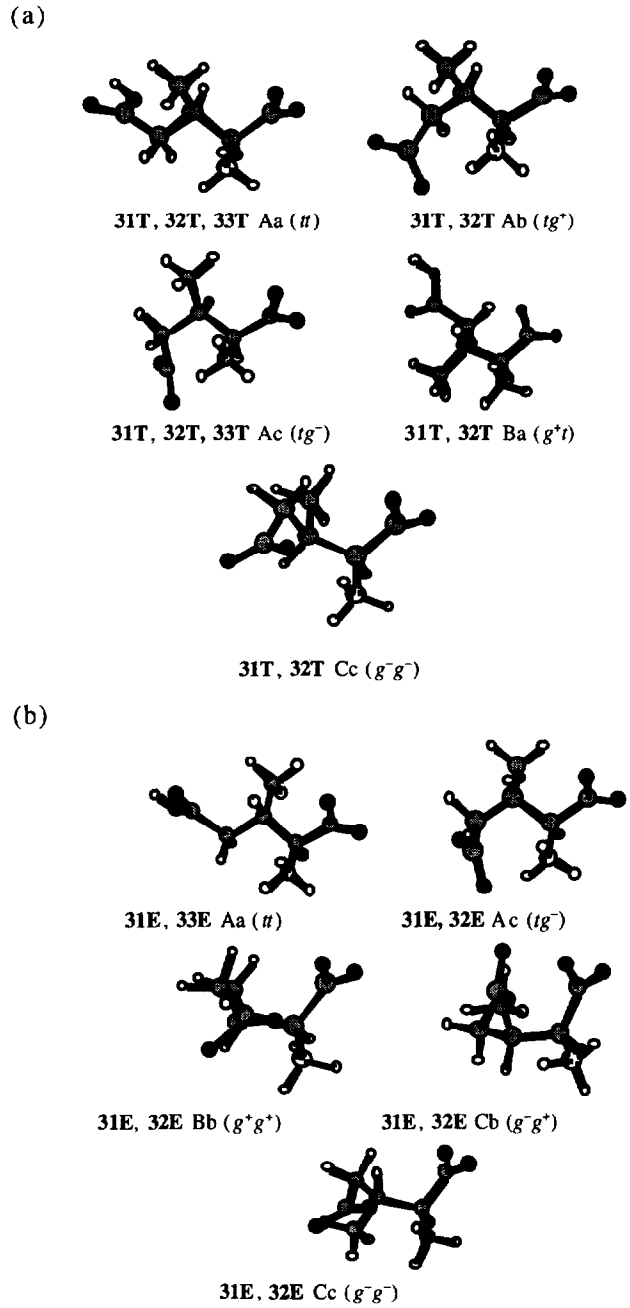

Figure 4. Achieved major conformations for the two (**3T–3E**) glutamate analogues at different pH by MD (a) five conformations of **3T**: Aa, Ab, Ac, Ba, Cc; (b) five conformations of **3E**: Aa, Ac, Bb, Cb, Cc. (The first number indicates the position of the methyl or methylene (at carbon **3** or **4**), the second one the predominant form in the pH zone considered (isoelectric zone **1**, neutral zone **2**, and alkaline zone **3**) the letter **E** or **T** the relative configuration of the methyl and **M** the methylene substituent.)

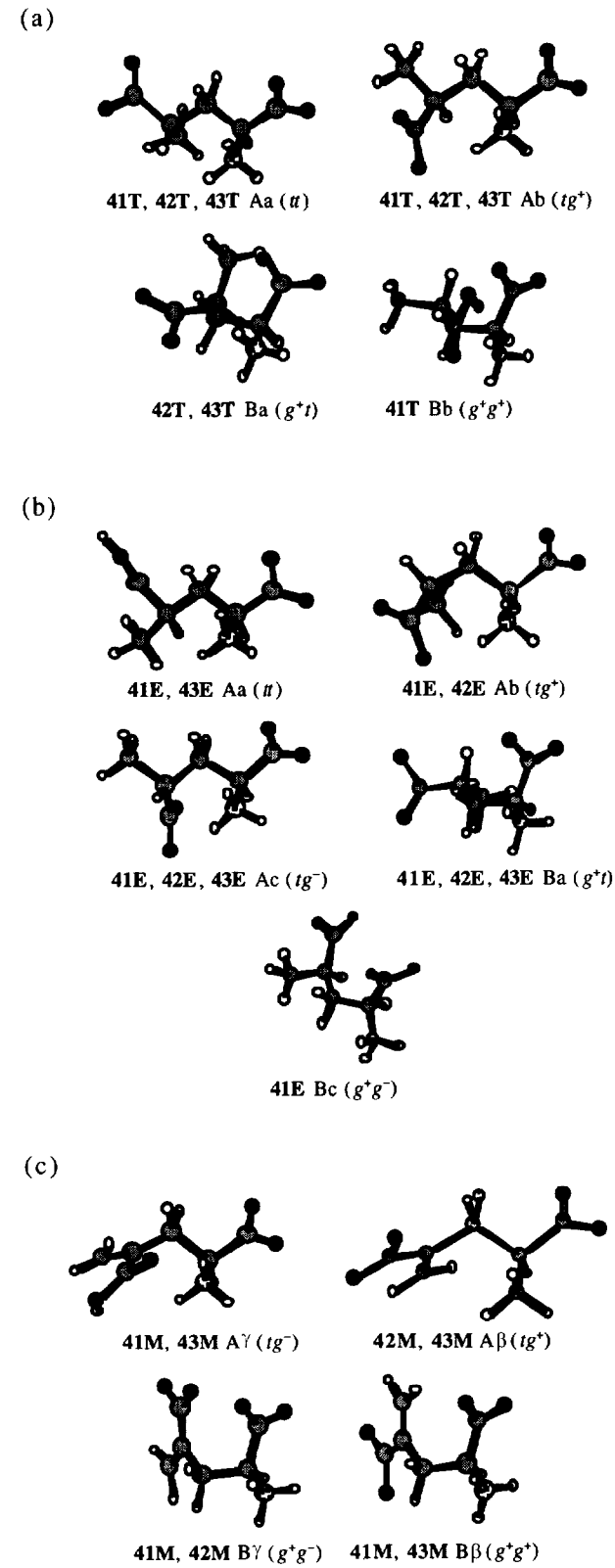

Figure 5. Achieved major conformations for the two (**4T–4M**) glutamate analogues at different pH by MD (a) four conformations of **4T**: Aa, Ab, Ba, Bb; (b) five conformations of **4E**: Aa, Ab; Ac; Ba, Bc; (c) four conformations of **4M**: Aγ, Aβ; Bγ; Bβ. (The first number indicates the position of the methyl or methylene (at carbon **3** or **4**), the second one the predominant form in the pH zone considered (isoelectric zone **1**, neutral zone **2**, and alkaline zone **3**), the letter **E** or **T** the relative configuration of the methyl and **M** the methylene substituent.)

and afterwards the study was developed at neutral pH in a box filled with water molecules (Fig. 3) and the relative dielectric constant was set to $\varepsilon = 1$. The structures found to have ratios up to 10% will be considered representative of the different NMR solutions. For each compound, we have analysed numerous MD simulations and Table 2 only presents the best protocol for each compound, at three pH values.

We observed a good agreement between the experimental NMR and the MD results, versus the best protocol for each compound, as shown in Figure 6. From the various solutions resulting from the MD approach (Table 2), one set for each isomer presented good agreement with the populations of rotamers obtained from NMR spectra (Table 1 and Fig. 6a) and, especially, with the calculated vicinal $^3J_{^1H,^1H}$ coupling constants and long-range heteronuclear $^3J_{^{13}C,^1H}$ coupling constants (Table 3 and Fig. 6b). Many of the conformational properties like J-couplings are not linearly related to the conformations and need to be calculated for each structure and then averaged (Table 3). By using P_i, the fractional population for each ith conformational microstate, the average coupling constant can be computed from the following:

$$^3J_{(HH)} = \Sigma P_i * {}^3J_{i(HH)} \quad (5)$$

$$^3J_{(HC)} = \Sigma P_i * {}^3J_{i(HC)} \quad (6)$$

The coupling constants were calculated from the corresponding dihedral angles of each conformer generated by molecular dynamics (Table 3).

Experimental values (Table 1) are discussed with regard to the calculated values from the conformational equilibrium possible in solution and generated by MD. In Table 3 and in Figure 6b, the $\Sigma(J_{calc} - J_{exp})$ evaluated from about 10 coupling constants ($J_{H,H}$ and $J_{C,H}$) for the conformer populations generated for each compound show that solution averaging is well described in agreement with the NMR data.

The protocol with the presence of water molecules seems to be generally the appropriate experiment for **3T**, **4T**, **4E**, and **4M** since good agreement is observed with the NMR results (Fig. 6). The decreased correspondence for **3E** indicates a difficult compromise between the steric effects and any intramolecular stabilizing forces, and thus suggests a relative modification of the force field. So, if we reduce the electrostatic contribution on **3E** by removing one formal charge (i.e. on the the γ-carboxylate group), we conceive a protocol on **3E** at isoelectric pH (**31E**) with functional groups γ-CO_2H, α-CO_2^- and α-NH_3^+ during 200 ps at 300 K ($\varepsilon = 5$). The calculated coupling constants are then in an improved agreement with the NMR experimental data for this isomer (Table 3 and Fig. 6).

The 'A' (t) orientation [α-CO_2^-–C(2)–C(3)–C(4)] (170°) is observed in the MD generated conformations and in the NMR structures of **3T**, **4T**, and **4E** while the 'C' (g^-) orientation of the angle [α-CO_2^-–C(2)–C(3)–C(Me)] (170°) is favoured by a different steric interaction in the **3E** structure. In **4M** solution, where the double-bond character of the methylene moiety ensures a planar group, theoretical and solution results agree with the 'B' (g^+) orientation [α-NH_3^+–

Table 3. Homonuclear ($^1H,^1H$) and heteronuclear ($^{13}C,^1H$) coupling constants of the five isomers calculated with the MD protocol which have a good correlation with the NMR results

	^3J (Hz)											
	3T		**3E**			**4T**		**4E**			**4M**	
	31T[a]	**32T**	**31E**[a]	**32E**		**41T**[a]	**42T**	**41E**[a]	**42E**[b]		**41M**[a]	**42M**[a]
2,3	6.5	4.1	4.7	4.7	2,3a	6.8	10.2	5.1	5.3	2,3a	5.4	4.5
3,4a	6.6	5.3	5.0	5.0	2,3b	6.1	3.3	7.9	8.1	2,3b	8.2	8.9
3,4b	6.8	7.2	7.3	7.3	3a,4	7.7	9.3	8.1	7.4	2-H,4-C		3.0
4a-H,2-C		3.8		3.7	3b,4	4.4	4.4	4.8	5.2	3a-H,1-C		4.6
4a-H,3Me-C		3.6		4.0	4-H,2-C		3.3		3.5	3a-H,5-C		3.7
4b-H,2-C		3.8		3.7	2-H,4-C		3.2		3.0	3a-H,6-C		3.4
4b-H,4Me-C		2.6		2.5	3a-H,1-C		1.8		3.1	3b-H,1-C		2.9
2-H,4-C		3.3		4.2	3a-H,5-C		3.1		3.5	3b-H,5-C		4.8
2-H,3Me-C		5.1		4.0	3a-H,4Me-C		2.6		2.7	3b-H,6-C		5.3
					3b-H,1-C		3.1		2.8			
					3b-H,5-C		4.2		3.8			
					3b-H,4Me-C		3.3		3.7			
$\Sigma \Delta J_{HH}$ MD/NMR	5.6	6.3	3.8	7.3		3.6	13.8	2.0	7.9		1.7	6.6

[a]Heteronuclear ($^{13}C,^1H$) coupling constants in acidic and basic solution are difficult to measure.
[b]Protocol 2: 34% Ab + 22% Ac + 22% Ba + 22% Cc
For each i the conformational microstate, the average coupling constant can be computed from:

$^3J_{(HH)} = \Sigma P_i * {}^3J_i$ (HH)

$^3J_{(HC)} = \Sigma P_i * {}^3J_i$ (HC)

$[J_{2,3a} = 34\% * J_{2,3a}$ (**Ab**) $+ 22\% * J_{2,3a}$ (**Ac**) $+ 22\% * J_{2,3a}$ (**Ba**) $+ 22\% * J_{2,3a}$ (**Cc**) $= 5.3$ Hz $(J_{obs} = 4.5)]$

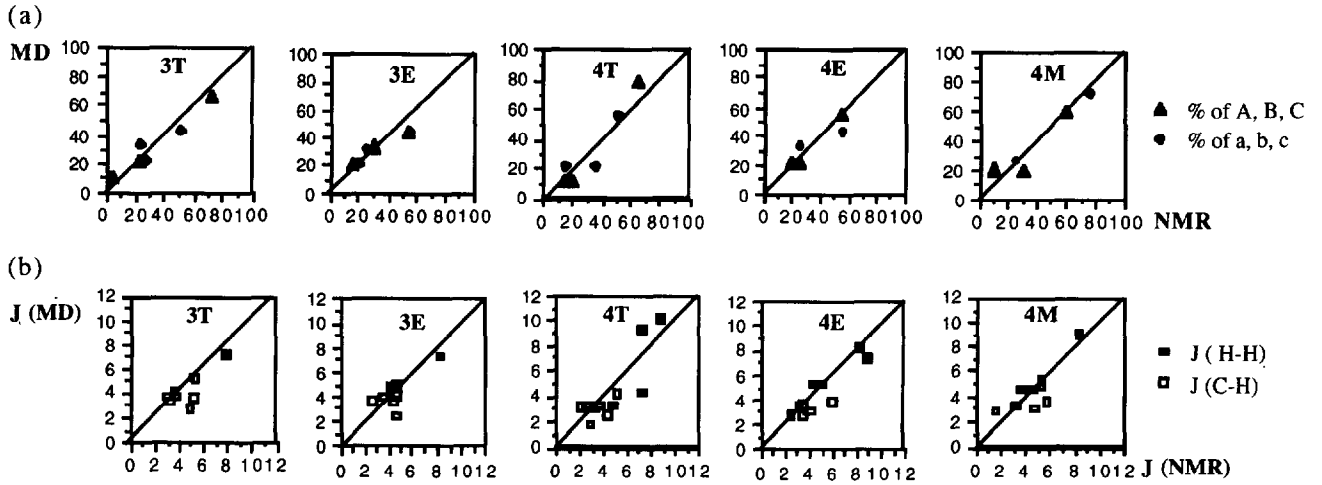

Figure 6. (a) Correlation between the observed (NMR) and calculated (MD) probabilities of the rotamers of the five isomers (**3T**, **3E**, **4T**, **4E**, and **4M**) and (b) between the experimental (NMR) and calculated (MD) coupling constant using the MD runs that present the best correspondence in the population of rotamers between MD and NMR data.

C(2)–C(3)–C(4)] (170°), despite intramolecular forces not being well defined.

Although one conformation is always favoured for these five studied amino acids, a range of conformations is clearly available to the molecules in solution. The MD data show the following conformational preferences in D_2O solution at pH 7: Ab, Ac, and Cc for **32T**, Ac, Bb, Cb, and Cc for **32E**, Ab for **42T**, Ab, Ac, Ba, and Cc for **42E**, and Aβ and Bγ for **42M** (Figs 4 and 5).

At pH 3, when the γ-CO_2^- carboxylate group is protonated, an interaction (like a hydrogen bond) is established with the α-CO_2^- and some conformers which were minor at pH 7 are now favoured such as Bb: Aa, Ba, and Bb for **31T**, Aa, Bc, and Ca for **31E**, Aa, Ac, and Bb for **41T**, Bc and Cb for **41E**, and Aγ and Bβ for **41M** (Figs 4 and 5). At alkaline pH, the '**a**' conformer with the two carboxylate groups 'extended' is predominant. The preferred conformation of the unprotonated molecule is the sterically favoured one, Aa showing a large zig-zag alkylamine chain ending in a carboxylate group, or Ba, corresponding to a large 'W' between the amino and the carboxylate groups.

The predominant conformations at different pH values (Fig. 6) are in agreement with the experimental NMR data (Table 3). This agreement probably arises because the calculations have included the charge and the hydration effects of the aqueous solvent.

Structural characteristics of these ligands. To explore structural features responsible for the pharmacological properties of the ligands, we performed the calculations under similar conditions (i.e. same solvent) as those under which the experimental results were obtained. It is found that for activity similar to that of glutamate, the positively charged N atom and two acidic groups are necessary. However, it will be noted that on the receptor a negatively charged moiety with proton donor abilities could be necessary, thus each of the interacting atoms may establish multiple interactions with the atoms of the receptor. A conformational study was performed at neutral pH and at isoelectric pH of the zwitterionic molecule, in order to propose a different ligand conformational state that could play a key role in the efficiency of the interaction including hydrogen-bonds. Consistent with the literature, data that argue against a charge delocalization between both oxygens of the γ-acid and in favour of a specific hydrogen bond between the distal acidic hydroxyl and the receptor, compounds **31** and **41** were built and analysed by MD. The ionized functional groups now become γ-CO_2H, α-CO_2^-, α-NH_3^+ and may supply the system **32** or **42** with energy (to pass conformational barriers), to generate other conformers. In a model bound to the receptor by a proton donor or a water molecule, the resulting conformations may be characterized by different internuclear distances between Nα, Cα, Cγ.[18b]

The conformational and the electrostatic energy term were generally the most significant classification criteria. We have also compared the five structures in terms of dihedral angles χ_1 [α-CO_2–C(2)–C(3)–C(4)] and χ_2 [C(2)–C(3)–C(4)–γ-CO_2^-] corresponding to their relative flexibilities. The MD run at 300–600 K in a water box favoured during the trajectory some 'less-staggered' rotamers that represent high-energy intermediates neighbouring to the transition state. They are almost in an 'eclipsed' form represented by the symbol (*) with a ±80–115 *gauche* torsion angle instead of ±60° or with a ±125–155° *trans* torsion angle instead of ±170° according to the staggered rotors χ_1 and χ_2. They represent a particular transition state implied in the interconversion of rotamers: A→A*→B*→B or a→a*→b*→b. The presence of water molecules favoured these constrained structures, with the four isomers **3E–4T**.

Rather than classify the conformational populations by combination of symbols *t* and *g* they are grouped in a

second step into a limited number of classes (I–IV) according to the distance (d_1) between the positively charged N atom and the carbon atom of the γ-CO_2^- group, but pairs with the same $^+$N—γCO_2^- distance will differ in the distance between carboxylate groups (d_2). Two groups are considered in electrostatic interaction if their distance is less than (or equal to) 4 Å.

Type I like Ab displays an attractive electrostatic potential between the α-NH_3^+ and γ-CO_2^- groups in a folded structure and thus corresponds to the shortest distance d_1 [d_1(α-NH_3^+–γ-CO_2^-) < 4 Å] between these two functional groups. Type II like Aa is characterized by the greatest distance d_2 between the functional groups with the same charges α-CO_2^- and γ-CO_2^- [d_2(α-CO_2^-–γ-CO_2^-) > 4.5 Å]. Meanwhile, the distance d_1 remains relatively small. Type III like Ba or Bb is characterized by a long distance d_1 [d_1(α-NH_3^+–γ-CO_2^-) > 4 Å] and a relatively short distance d_2 between the α-CO_2^- and γ-CO_2^-. Finally, type IV like Bc is characterized by the shortest distance between the two carboxyl groups [d_2(α-CO_2^-–γ-CO_2^-) < 3.5 Å]. These two last structures become more stable at pH 3, since the protonation of the γ-carboxyl group creates hydrogen bonding with α-CO_2^-. It results in a close proximity of the two groups. At isoelectric pH, an electrostatic attraction between the 3-carboxy and the 1-carboxylate axial groups, led to 'folded' structures characterized by a short distance d_2 between the two carboxyl groups and belonging to the Type IV or to the type III.

These four families (types I–IV) are essentially characterized by the above-mentioned values of the two interatomic distances (Å) d_1 and d_2, but other families (types I′–IV′) with the same d_1 and d_2 distances will differ in the alkyl chain by the torsion angles χ_1, χ_2 (g^-) (Table 4). Ring closure in the ACPD isomers and in the KA molecule does not allow these last types (I′–IV′). They correspond to different conformations: Cc and Cγ (type I′), Ca (type II′), and Cb, Cβ (type IV′).

To gain more insight into the relative orientations of conformers described above, these features are evaluated (Figs 7–13; Tables 4 and 5) for the studied compounds (**3T–4M**). It is possible to assume that the conformer that binds to glutamate receptors resembles one of the stable conformers in aqueous solution. On the basis of the conformation–activity studies of known agonists, it should be possible to extract a binding conformation of glutamate to a subtype receptor.

Conformational similarities of the five studied compounds were evaluated by calculating the root mean square (rms) deviation between heavy atoms after superimposition. The results represent groups of structures whose small RMS deviations (< 0.5 Å) suggested that they may belong to the same conformational family, even though some superimpositional discrepancies occured on the alkyl chain.

Comparison with a specific metabotropic agonist; (1*S*,3*R*)-*trans*-ACPD)

The five compounds have been tested on the 'mGluR$_{1a}$' receptor (metabotropic receptor) and only the [(2*S*,4*S*)-4-methylglutamic acid] **4T** exhibited an activity

Table 4. Torsion angles χ_1 [α-CO_2 –C(2)–C(3)–C(4)] and χ_2 [+NC(2)–C(3)–C(4)–γCO_2^-] and interatomic distances of specific agonists of the metabotropic receptors (Å). The maximal and minimal permissible distances: d_1 between the terminal carboxyl carbon and the nitrogen (αNH_3^+—γCO_2^-) and d_2 between the two carboxyl carbon atoms (αCO_2—γCO_2).

Compounds	d_1		d_2		χ_1		χ_2		Family (rms)[d]
	min	max	min	max	min	max	min	max	
trans ACPD[a]	2.9	5.0	4.6	5.2	78.2	162.5	70.2	168.1	I, II, III
Conformations[b,c]	d_1		d_2		χ_1		χ_2		
4T									
Ab	3.2		4.7		164.3		67.3		I (0.176)
Ab*	3.2		4.8		170.3		83.5		I (0.137)
A*b	3.8		5.0		134.0		90.8		I (0.171)
Aa	4.5		5.2		171.8		166.0		II (0.334)
A*a*	4.3		5.3		142.3		141.3		II (0.166)
A*a	4.4		5.2		149.8		156.2		II (0.221)
Ba	4.9		4.8		77.4		161.6		III (0.095)
Bb	4.4		4.2		76.6		69.1		III (0.448)
Ba*	4.8		4.9		81.7		142.1		III (0.096)
B*a	4.7		5.2		118.7		155.9		III (0.217)

[a]The two distances (d_1 and d_2) and the torsion angles χ_1 and χ_2 are obtained for the different *envelope* forms for the cyclopentane.[17]
[b]We have represented the conformations of the **4T** isomer that have d_1, d_2, χ_1, and χ_2 contained between the minimum and the maximum values obtained for the (1*S*,3*R*) *trans*-ACPD.
[c]With the solvation box during the MD experiment (300 K jump to 600 K), some conformations are in an 'eclipsed' form and represented by the symbol '*'.
[d]RMS deviation between heavy atoms for the (**I**, **II**, **III**) family of (1*S*,3*R*) *trans*-ACPD and the structure of **4T** so that they may belong to the same family.

similar to glutamate. The (1*S*,3*R*)-*trans*-ACPD also activates the metabotropic subtype 'mGluR$_{1a}$' receptor.[8] The conformational requirements of mGluRs were based on the structure–activity relationship of the known mGluRs agonist (1*S*,3*R*)-*trans*-ACPD (Table 4).

The (1*S*,3*R*)-*trans*-ACPD analogue adopts multiple conformations and it belongs to the conformational classes I [χ_1 (120–165: A, A*); χ_2 (75–105: b, b*); d_1 (2.87–3.64); d_2 (4.55–5.01)], II [χ_1 (90–145: B*, A*); χ_2 (120–150: a*); d_1 (4.15–4.58); d_2 (4.76–5.22)], and III [χ_1 (78–98: B*); χ_2 (140–168: a*, a); d_1 (4.76–4.96); d_2 (4.72–4.83)]. These three families may be in qualitative agreement with the active form[17] (Fig. 7). In this agonist, the C(2)–C(3) and C(3)–C(4) rotors cannot adopt a g^--C and g^--c conformation, respectively. The (1*S*,3*R*)-*trans*-ACPD can be considered an interesting tool for investigations on molecules such as **4T** with approximately the same activity.

The analogue **4T** belongs mainly to the family I (60%) at pH 7 with the conformer tg^+-Ab (and also Ab*, A*b*). The 4-methyl-glutamate **4T** showed a remarkable substituent effect on the increased energy difference between the global minimum energy Ab and other conformations. This allows us to conclude that high rotational barriers have to be passed for the **4T** isomer to obtain the different conformations which participate in the solution. An energy gap of 3.5–12.3 kcal mol^{-1} could be evaluated between **42T** tg^+-Ab and the values obtained for the other conformers. Clearly, the **42T** Ab conformation appears to be particularly stable. The electrostatic interaction between the α-NH_3^+ and the γ-CO_2^- groups at neutral pH (**42T**) stabilized the Ab conformation and so the family I. The 'extended' conformation *tt*-Aa (and also A*a, A*a*) belongs to the family II and represents a minor conformer in the neutral **4T** solution, but is essentially present in the alkaline **43T** solution. The steric factor will influence a ligand to adopt the less constrained

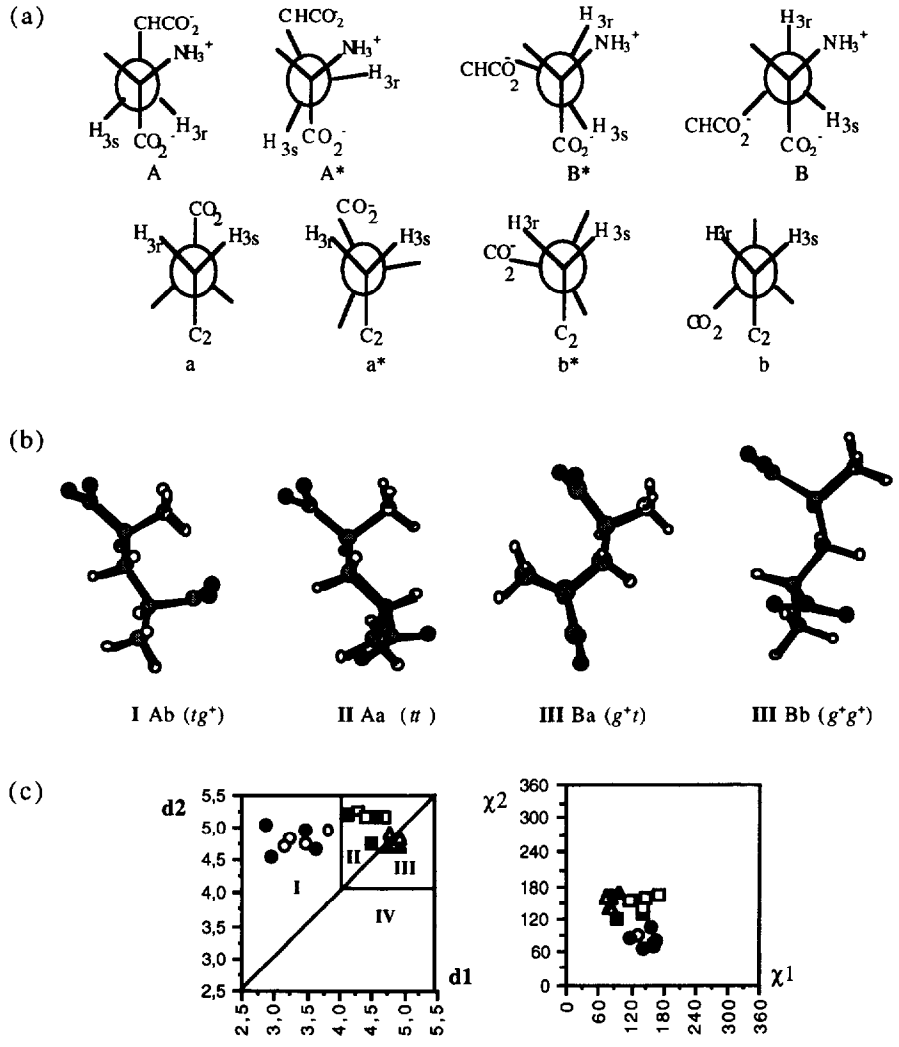

Figure 7. (a) Newmann projection of the different **4T** rotamers similar to those of *trans*-ACPD; (b) Representation of the different conformational families **I**, **II**, and **III** corresponding to Ab, Aa, and Ba (or Bb), respectively; (c) Representation in a diagram of the three conformational families **I–III** for the **4T** isomer and the (1*S*,3*R*)-*trans*-ACPD according to their characteristic distances d_1 (α-NH_3^+–γ-CO_2^-), d_2 (α-CO_2^-–γ-CO_2^-) and their characteristic torsion angles χ_1 [αCO_2–C(2)–C(3)–C(4)] and χ_2 [$^+$NC(2)–C(3)–C(4)–γCO_2^-] (Table 4). *trans*-ACPD: ● I; ■ II; ▲ III; ◆ IV; **4T** isomer: ○ I; □ II; △ III; ◇ IV.

conformation *tt*-Aa (Family II). The family III corresponds at pH 7 to the higher energy structure g^+t-Ba (and also B*a*, B*a) with total energies 4–6 kcal mol^{-1} greater than the lowest-energy conformer. Family III participates a little (10%) in the neutral solution of **4T** but at pH 3, when the protonation occurs for the γ-CO_2^- group, this type of family increases (40%) with **41T** g^+g^+-Bb (Fig. 5).

The present results, indicating that **4T** was a potent agonist of $mGluR_{1a}$, support our proposed hypothesis, while the metabotropic active conformations of glutamate only concerns the families (I–III) according to the *anti* (*t*) and *gauche* (g^+) C(2)–C(3) and C(3)–C(4) bonds (Table 4). Among the forms of glutamate, the four ones *tt*-Aa, tg^+-Ab, g^+t-Ba and g^-g^+-Bb and also the 'less-staggered' or intermediate rotamers (represented by the symbol *) A*b*, A*a*, B*a*, fitted well for each of the (1*S*,3*R*)-*trans*-ACPD I, II, and III families (Table 4; Figs 7 and 8).

Figure 8 shows the superimposition of the three conformational classes I, II and III of (1*S*,3*R*) *trans*-ACPD compound in qualitative agreement with the three types of the potential active residue arrangement Types I (Ab, A*b*), II (Aa, A*a*), and III (Ba, B*a* and Bb) of the **4T** isomer (RMS of deviation between heavy atoms <0.16 Å, Table 4). This illustrates the fact that the conformation at the receptor binding site might be relevant to one (or more) of these structures.

It is interesting to note that only **3E** can exist in a predominant g^+g^+-Bb conformation (family III), a minor tg^+-Ab conformation (family I) and can also adopt the extended *tt*-Aa conformation (family II) representing its major form at basic pH. At the same time, **3E** weakly activates the metabotropic subtype '$mGluR_{1a}$' receptor (less than **4T** and (1*S*,3*R*)-*trans*-ACPD) with an estimated EC_{50} value of 10–100 μM (for reference, L-Glu and **4T** compounds gave a value of 1–10 μM in this assay).

Comparison with a specific ionotropic KA agonist (kainic acid)

Only the analogues with a methyl group at the 4-position have been tested on the ionotropic KA receptor and the [(2*S*,4*R*)-4-methylglutamic acid] **4E** was identified as having exceptional selectivity for KA receptor subtype comparable to kainic acid itself.[21]

The conformation of kainate using ^1H NMR has not yet been totally elucidated. Thus, for a classical structure–function relationship study, we have undertaken a molecular modelling and NMR study of kainic acid.[23] The C(2)–C(3) rotor cannot adopt a g^--C conformation corresponding to χ_1 [α-CO_2^-–C(2)–C(3)–C(4)] $= -60°$, because the five-membered ring structure of kainic acid does not allow this torsion angle. Thus, the carboxy group on C(2) and the carboxymethyl group on C(3) can adopt conformations corresponding only to a fluctuating angle χ_1, C(2)–C(3) between 70° and 170° (B, B*, A*, A). Among the three forms (t, g^+, and g^-) concerning the χ_1 conformation [C(1)–C(2)–C(3)–C(7)] of the glutamate, the angle values found for KA characterize one rotamer between gauche B (g^+) and antiperiplanar A (t) conformations. On the other hand, the ring of kainate can adopt flexible forms of pseudo rotational circuit of cyclopentane [10 *envelope* **E** and 10 *half-chair* **T** conformers (Fig. 9), but the presence of the three substituents will give rise to an induced potential energy barrier opposing free pseudorotation. The molecular modelling calculations on kainic acid (zwitterion) were performed on the 30 *envelope* conformations resulting from the combination of the rotamers 'A, A*, B*, and B' about χ_1, and the three rotamers 'a, b, and c' about χ_2. The final structures obtained after several mechanics and dynamics molecular calculations with the introduction of explicit water molecules in a solvation box are represented (Fig. 9) by external point of dotted radials in the pseudorotational circle. These conformations (*tt*-A*a, tg^+-A*b, tg^--A*c and g^+t-B*a, g^+g^+-B*b, g^+g^--B*c) corresponding to the seven envelopes from E_3 to E_4 (Fig. 9) were examined for the overall energetic favorability and compared with the structure derived from the NMR data. The torsion

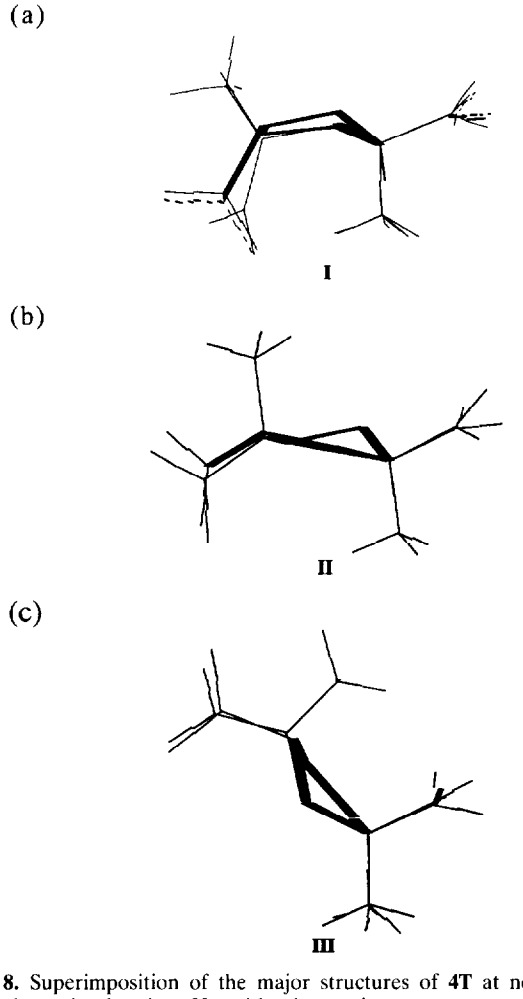

Figure 8. Superimposition of the major structures of **4T** at neutral pH and at isoelectric pH, with the major structures of the (1*S*,3*R*)-*trans*-ACPD represented by the *envelope* conformations and belonging, respectively, to (a) family I (E_1) and **42T** Ab*, (b) family II (^5E) and **42T** A*a*, and (c) family III (E_2) and **42T** Ba.

angles of these generated structures can be correlated to the corresponding coupling constants by using Karplus-type equations.

Our observed NMR values ($^3J_{H(2)H(3)}=2.6$ Hz; $^3J_{H(2)C(4)}=4.0$ Hz, and $^3J_{H(2)C(7)}=4.7$ Hz) should include an almost exclusive participation (>90%) of conformer A* ($\chi_1=120$–$150°$) characterized by the calculated values ($^3J_{H(2)H(3)}=2.3$ Hz; $^3J_{H(2)C(4)}=4.0$ Hz, and $^3J_{H(2)C(7)}=5.4$ Hz). A difference of 0.5 Hz compared with the calculated values, although not really larger than the experimental error (0.2–0.3 Hz) may be interpreted as a slight contribution (<10%) of the conformer B* ($\chi_1=90$–$120°$) represented by the calculated values $^3J_{H(2)H(3)}$ (10.1–12.0 Hz), $^3J_{H(2)C(4)}$ (2 Hz), and $^3J_{H(2)C(7)}$ (2.5–4.2 Hz).

The NMR data ($^3J_{H(2)H(3)}=2.6$ Hz, $^3J_{H(2)C(4)}=4.0$ Hz, and $^3J_{H(5a)C(3)}=5.2$ Hz) showed that the predominant A* conformation adopts the ^{4}E envelope characterized by the calculated values ($^3J_{H(2)H(3)}=2.3$ Hz, $^3J_{H(2)C(4)}=4.0$ Hz, and $^3J_{H(5a)C(3)}=5.8$ Hz) while the minor B* conformer was found in the ^{5}E envelope represented by the calculated values ($^3J_{H(2)H(3)}=5.3$ Hz, $^3J_{H(2)C(4)}=1.8$ Hz, and $^3J_{H(5a)C(3)}=0.5$ Hz).

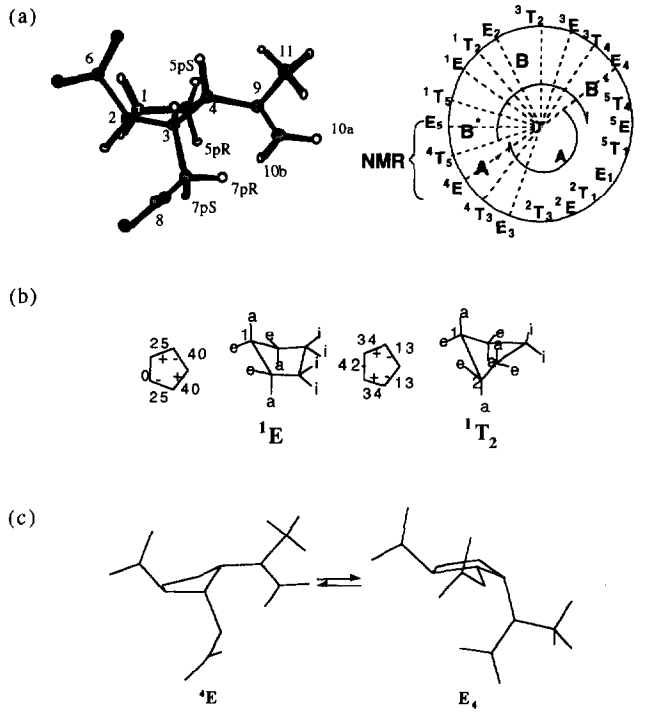

Figure 9. (a) Structure of the kainic acid at neutral pH: *envelope* conformation ^{4}**E** for kainic acid at pH 7. Pseudorotational pathway of the cyclopentane ring. Each external point of dotted radials in the circle represents a specific **E** form or **T** conformation generated by MD. (b) Considered conformations for cyclopentane. The forms, *envelope* **E** and *half-chair* or *twist* **T** are represented in perspective drawing, as well as in the conventional formula indicating the approximate value of the torsion angles and their sign and with the following types of exocyclic bonds: *equatorial* (*e*), axial (*a*), and the so-called *isoclinal* (*i*) bonds. The former has four carbons in the same plane, in contrast, the half-chair has three coplanar carbon atoms, one above and one below (^{1}**T**$_2$), (c) Conformations envelope **E** for kainic acid at pH 7. Conformational equilibrium between the structure ^{4}**E** and another *envelope* **E**$_4$ when the out-of-plane carbon C-4 is pushed down.

The molecular modelling calculations and the experimental NMR value strongly suggested that the conformational requirement of kainic acid (zwitterion) is a major eclipsed A* χ_1 [α-CO_2^-–C(2)–C(3)–C(4)] (120–150°) or possibly B* ($\chi_1=90$–$120°$) as the ring does not allow the very extended *t*-A rotamer (150–170°) and less still the *g*-B one (70°) (Table 5).

For the second torsion angle χ_2, the ^3J ^{13}C–^{1}H coupling constants and the NOE experiments allow us to determine the assigment of the diastereotopic CH_2(7) protons and the major g^--c rotamer population in solution with a little participation of the *t*-a rotamer. The observed values $^3J_{H(3)H(7a)}$ (6.7 Hz), $^3J_{H(7a)C(2)}$ (6.0 Hz), $^3J_{H(3)H(7b)}$ (8.7 Hz), and $^3J_{H(7b)C(2)}$ (3.7 Hz) showed that the H(7a) and H(7b) are *proR* and *proS*, respectively, and that the g^--c rotamer is predominant (60%).

The preferred conformations can belong to several families (Fig. 10), the major one I′ with tg^--A*c and the minor ones including (a) the family I with tg^+-A*b, (b) the family II with *tt*-A*a, (c) the family III with the g^+t-B*a and g^+g^+-B*b conformations, and (d) the family IV with g^+g^--B*c conformation.

In view of the biological activity, we can compare these results to those obtained for the **4E** isomer (Table 5). An identical set of families represents the **4E** solution at neutral pH (Fig. 10): the major conformation tg^--Ac belonging to the family I′ and the same ensemble of minor conformers like tg^+-Ab (family I) and g^+t-Ba (family III), which represent 20% of the **42E** solution. The g^+t-Ba (family III) conformation is sterically favoured for the unprotonated molecule **43E**, while at pH 3 this family is present in small amounts as the protonation of the distal acid induced a slight contribution of the conformation g^+g^--Bc (family IV) in **41E** solution.

Figure 11 shows the superimposition of the conformational classes of kainic acid compound in qualitative agreement with the four types of the potential active residues arrangement of **4E** isomer (RMS of deviation between heavy atoms ≤ 0.4 Å, types I′ (Ac and A*c), I (Ab and A*b), III (Ba and B*a), and IV (Bc and B*c). This illustrates the fact that the conformation at the receptor binding site might be relevant to one (or more) of these structures. The tg^--Ac conformation is observed to be specific of this ionotropic KA receptor as of **4E** (and **3T**).

The predominant conformations of the (2*S*-3*R*)-3-methylglutamic acid, **3T** at different pH values are similar to those of **4E** in the following families: I′ (Ac), I (Ab), and III (Ba and Bb). It would be interesting to verify for the **3T** isomer whether this similarity induces identical neurobiological activity on the ionotropic KA receptor, as the 3-methylglutamic acid isomers have not been tested on this receptor. Four configurational isomers of 3-benzylglutamic acid, acyclic analogues of kainoids have been already synthesized in order to examine their pharmacological effects.[31] The (2*S*,3*R*)-3-benzylglutamic acid, with a similar configura-

tion to **3T**, presented the most potent neuroexcitatory activity, and its depolarizing activity was three times as potent as that of L-glutamic acid.

Comparison with a specific ionotropic NMDA agonist, (1*R*,3*R*)-*cis*-ACPD

Watkins et al. first proposed the conformational requirements of NMDA receptors to be a folded form of L-glutamate.[1] While the (1*S*,3*R*)-*trans*-ACPD isomer was recognized by metabotropic receptors, (1*R*,3*R*)-*cis*-ACPD was tested to be an effective agonist of NMDA receptors.[18] In a previous study,[16] a conformational analysis has shown that *cis*-ACPD adopts multiple conformations and it belongs to the conformational classes: II [χ_1 (122–163: A, A*); χ_2 (−142)–(−162): a, a*; d_1 (4.60–4.94); d_2 (4.63–5.06)] and IV [χ_1 (78–98: B, B*); χ_2 (−76)–(−108): c, c*); d_1 (4.56–4.90); d_2 (3.14–3.83)] (Table 5). At physiological pH, both carboxyl groups are found to be in an extended position (*tt*-Aa) to reduce the steric energy (type II). At isoelectric pH when the 3-carboxylate group is protonated, the *cis*-ACPD is represented by new privileged conformations. This isomer exhibits a conformation in which the 1-carboxylate group, α-CO_2^- is stabilized by an electrostatic interaction with the folded 3-carboxyl group, γ-CO_2H (type IV).

Since the *cis*-ACPD isomer was found to preferentially activate NMDA receptors, our previous study has provided clear evidence that A, A*, B*, B and a, a*, c*, c conformations correspond to the active rotamers of glutamate's C(2)–C(3) and C(3)–C(4) bonds (Fig. 12). Thus, the conformations of glutamate, *tt*-Aa (or A*a, Aa*) (family II) and g^+g^--Bc (or B*c, Bc*) (family IV) regarding the carbon chain are important factors for the NMDA (Fig. 12). These results led us to speculate further which rotamer would be an active form of glutamate by using *cis*-ACPD as template molecule.

Table 5. Torsion angles χ_1 [α-CO_2^-–C(2)–C(3)–C(4)] and χ_2 [+NC(2)–C(3)–C(4)–γCO_2^-] and interatomic distances of specific agonists of ionotropic receptors: the NMDA receptor (NMDA and *cis*-ACPD) and the kainate receptor (kainic acid). The maximal and minimal permissible distances: d_1 between the terminal carboxyl carbon and the nitrogen (αNH_3^+—γCO_2^-) and d_2 between the two carboxyl carbon atoms (αCO_2^-—γCO_2^-)

Compounds	d_1		d_2		χ_1		χ_2		Family (rms)[d]
	min	max	min	max	min	max	min	max	
kainic acid[a]	3.6	5.0	3.4	5.0	76.0	135.6	52.9	290.0 (−70)	I′, II, III, IV
(1*S*,3*S*)*cis*-ACPD[a]	4.6	5.0	3.1	5.1	78.2	162.5	197.9	283.5 (−76.5)	II, III, IV
NMDA[a]	3.1	3.8	3.3	4.0	76.2	287.0	—	—	

Conformations[b,c]	d_1	d_2	χ_1	χ_2	
4E					**4E/KA**
Ab	3.2	4.8	166.0	68.0	I (0.308)
Ac	3.6	4.6	183.6 (−176.4)	305.8 (−54.2)	I (0.394)
Aa	4.7	5.0	160.5	190.1 (−169.9)	II (0.193)
A*a*	4.6	5.1	145.8	154.4	II (0.274)
Ba	5.0	4.6	64.4	184.1 (−175.9)	III (0.067)
Bb	4.4	4.3	86.8	71.2	III (0.146)
Bc	4.7	3.4	83.0	288.2 (−71.8)	IV (0.235)
3T					**3T/KA**
Ab	3.0	4.6	159.2	66.8	I (0.236)
Ac	3.6	4.2	175.3	305.1 (−54.9)	I (0.334)
Aa	4.7	5.1	165.9	195.2 (−164.8)	II (0.213)
Ba	5.1	4.5	60.1	189.9 (−170.1)	III (0.108)
Bb	4.6	3.9	64.8	65.9	III (0.102)
4M					**4M/KA**
Bγ					
B*γ	4.9	3.8	70.4	251.7 (−108.3)	IV (0.285)
	4.9	3.9	88.4	259.1 (−100.9)	IV (0.249)
4M					**4M/*cis*-ACPD**
Bγ					
B*γ	4.9	3.8	70.4	251.7 (−108.3)	IV (0.114)
	4.9	3.9	88.4	259.1 (−100.9)	IV (0.086)

[a]The two distances (d_1 and d_2) and the torsion angles χ_1 and χ_2 are obtained for the different conformations of kainic acid, NMDA, and (1*S*,3*S*)-*cis*-ACPD.

[b]We have represented the conformations that have d_1, d_2, χ_1, and χ_2 contained between the minimum and the maximum values obtained for the kainic acid, NMDA, and (1*S*,3*S*)-*cis*-ACPD.

[c]With the solvation box during the MD experiment (300 K jump to 600 K), some conformations are in an 'eclipsed' form and represented by the symbol '*'.

[d]RMS of deviation between heavy atoms of the **4E** and **KA**; **3T** and **KA**; **4M** and **KA**; and **4M** with *cis*-ACPD.

Only a few isomers possess predominantly the g^+g^--Bc (family IV) conformation. Among the five studied analogues, only the major g^+g^--Bγ conformation, which is similar to the Bc conformation, belongs to the IV family and corresponds to 60% of **42M** solutions. It was demonstrated that the **4M** isomer presents a potent activity at ionotropic glutamate receptors (NMDA, kainate, and AMPA).[22] Thus, if we superimposed the three characteristic functional atoms α-N, α-C, and γ-C of the **42M** Bγ (or B*γ) and **41M** Aγ (and Bβ) with the major conformation of the (1*S*, 3*S*)-*cis*-ACPD, we observed a good agreement for the IV family (Fig. 13). Then we can conclude that this rotamer would be the most plausible conformation of glutamate required for binding to NMDA receptors in agreement with the pharmacophore suggested.[32] If this was not the case, this rotamer could be ruled out as the probable candidate and the conformation at the receptor binding site might be relevant to the II family.

Conclusion

This work has provided determination of ligand structures and the results underline the specificity of the influence of electrostatic and steric interactions for each compound. The conformation depends strongly on substitution, the solvent, and the pH. This aspect has to be considered, given the importance of a comparative study (NMR/MD) even for small charged molecules, in deciding which conformation is more populated than the other at a certain temperature in a specific solvent. We have introduced the solvent effect into our calculations and have carried out a rather complete investigation of it. It leads to the coexistence of a number of more or less extended forms in water in very satisfactory agreement with NMR solution findings. NMR parameters reflect the virtual conformation and at the same time the MD experiments are of great benefit in predicting the specific range of conformations available to each derivative in solution.

The conformations differ in the other compounds (**3T**, **3E**, **4E**, and **4M**) by the methyl (or methylene) position, that increases steric bulk and lipophilicity near the potential active groups. A different configuration of the methyl group corresponds in MD calculations to a loss of 2–3 kcal mol^{-1}. These modifications seem to be crucial for the ligand–receptor recognition mechanism. The biological activity of these derivatives

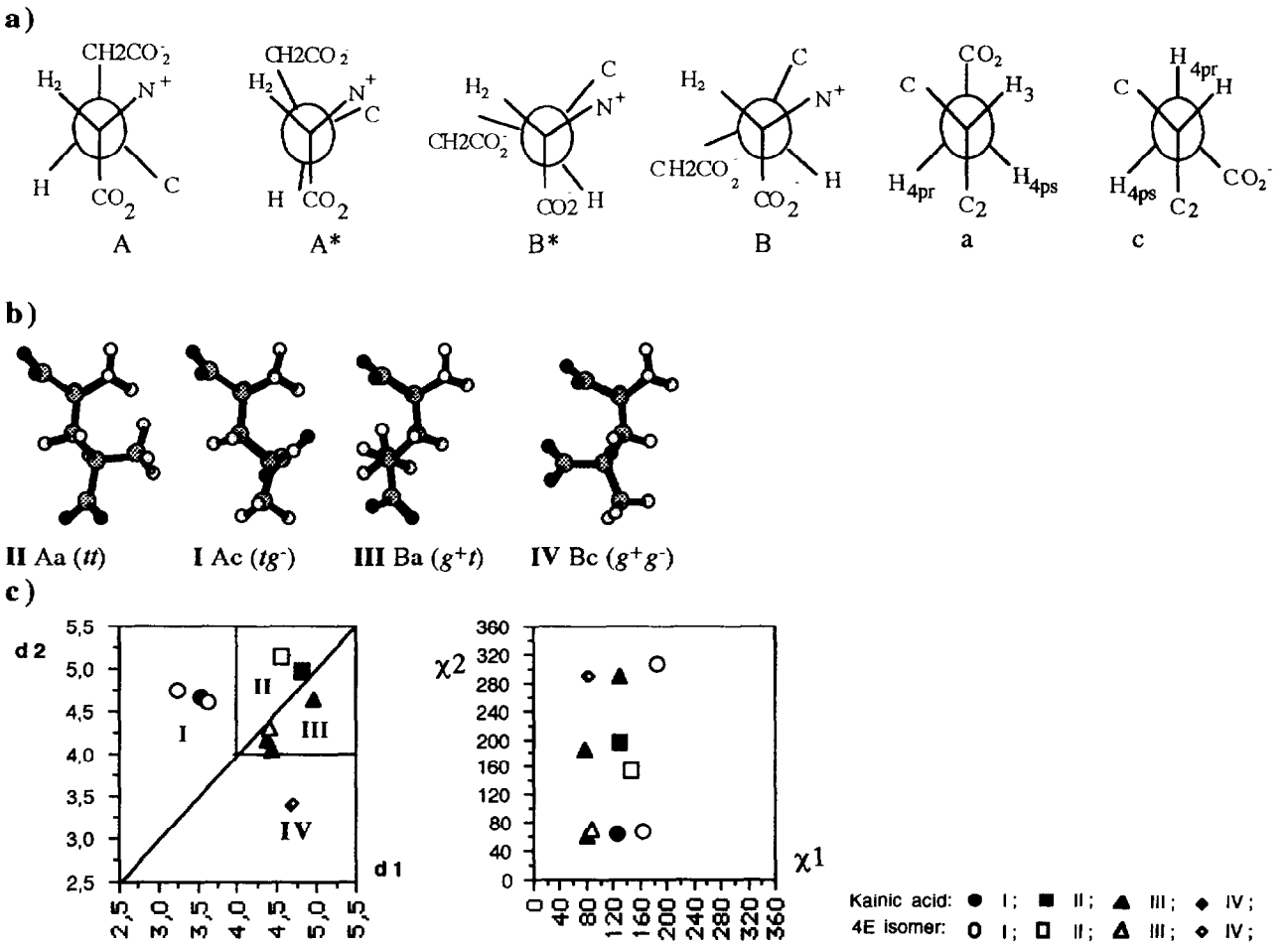

Figure 10. a) Newmann projection of the different **4E** rotamers similar to those of kainic acid. (b) Representation of the different conformational families (II, I, III, and IV) corresponding to Aa, Ac, Ba, and Bc, respectively, for the **4E** isomer. (c) Representation in a diagram of the four conformational families **I–IV** for the kainic acid and the **4E** isomer according to their characteristic distances d_1, d_2 and χ_1, χ_2 (Table 5).

depends on many factors, and these may include their conformation in solution.

The results of the present study reflect that **4T**, **4E**, and **4M** isomers selectively interact with high agonist conformation at different glutamate receptors of the central nervous system: **4T** at $mGluR_{1a}$ receptor, **4E** at the KA receptor, and **4M** at NMDA receptor, respectively. This makes **4T**, **4E**, and **4M** interesting tools for studies of conformational preferences of glutamate subtype receptors. Thus, the binding conformations of the metabotropic receptors correspond to the conformation *t*-A, g^+-B and *t*-a, g^+-b relative to the C(2)–C(3) and C(3)–C(4) torsion angle, respectively. In particular, the two *t*-A and g^+-b rotamers, predominant for the **4T** isomer, seem essential for the interaction at the $mGluR_{1a}$ receptor. While at the ionotropic receptor, the *t*-A, g^+-B and *t*-a, g^--c rotamers represent the active forms with a selectivity for the two subtype receptors as NMDA and KA receptors. When the *t*-A, g^--c activates the KA receptors, the g^+-B, g^--c conformation activates the NMDA receptors.

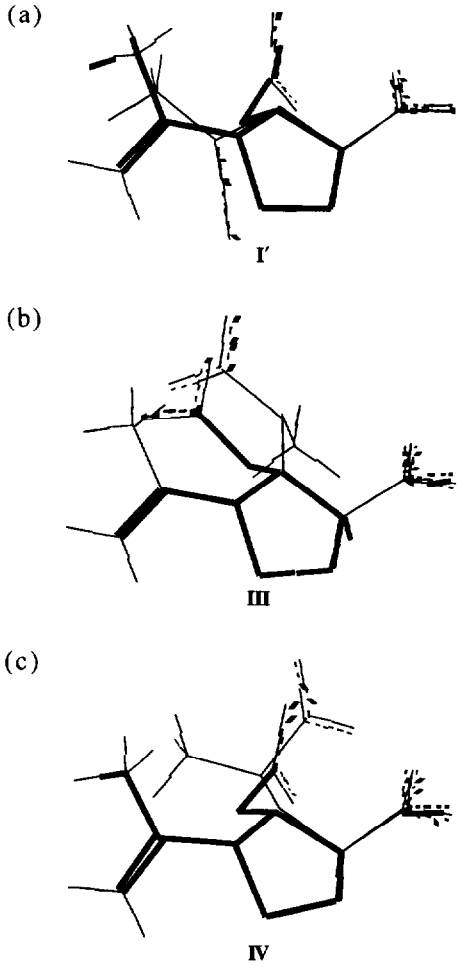

Figure 11. Superimposition of the major structures of **4E** at neutral pH, with the major structures of the kainic acid represented by the *envelope* conformations and belonging respectively to (a) the family I' (^{4}**E**) A*c and **42E** Ac, (b) the family III ($\mathbf{E}_5$) B*a and **42E** Ba, and (c) the family **IV** ($\mathbf{E}_5$) B*c and **42E** Bc.

Experimental

Biological activity

To examine the effect of the methyl or methylene derivatives[19] of glutamate on $mGluR_{1a}$, cRNA encoding this receptor was injected into *Xenopus* oocytes (1 ng per oocyte) as previously described.[20a] cRNA was synthesized in vitro as previously described with T3

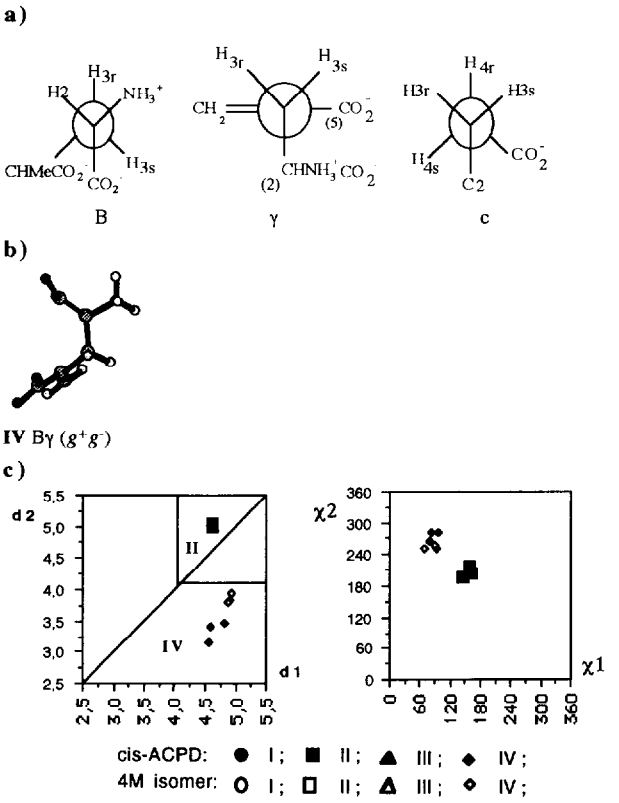

Figure 12. (a) Newmann projection of the different **4M** rotamers similar to those of (1*S*,3*S*)-*cis*-ACPD, whose enantiomer is a specific NMDA agonist. (b) Representation of the different conformational family IV corresponding to **B**γ for the **4M** isomer. (c) Representation in a diagram of the two conformational families II and IV for the (1*S*,3*S*)-*cis*-ACPD and the **4M** isomer according to their characteristic distances d_1, d_2 and χ_1, χ_2 (Table 5).

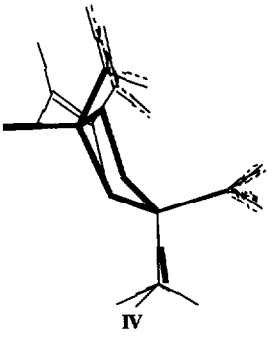

Figure 13. Superimposition of the major structure of **4M** at neutral pH, with the major structures of the (1*S*,3*S*)-*cis*-ACPD belonging to the family IV ($\mathbf{E}_5$) and **42M** B*γ.

RNA polymerase and using a plasmid DNA containing the entire $mGluR_{1a}$ cDNA as template.[20a] The activation of the Cl^- current was measured using the two electrode voltage-clamp procedure at a membrane potential of -70 mV.[20a]

Nuclear magnetic resonance

All NMR spectra were recorded on a Bruker AMX-500 spectrometer equipped with a X32 computer. A sample of **3T**, **3E**, **4T**, **4E**, and **4M** (7.4 mg) was dissolved in 0.6 mL of D_2O to give a final concentration 0.09 mol dm^{-3} for the different isomers. The pH (in fact pD = pH −0.4, uncorrected here) was adjusted by addition of DCl or NaOD. At pH 7 the samples have been dissolved in an aq NaD_2PO_4–Na_2DPO_4 buffer, and it was possible to attain concentrations of 0.09 mol dm^{-3} for the ^1H and ^{13}C experiments. The errors on the chemical shifts are 0.01 and 0.1 ppm for ^1H and ^{13}C, respectively. A crystal of 3-(trimethylsilyl)[2,2,3,3-$^2H_4$] propionic acid, sodium salt [$^2H_4$]TSP was used as internal reference for the proton shifts, and for the carbon a value of the absolute frequency was used. The coupling constants are given with a precision of 0.3 Hz. The spectrum simulation was done on a Macintosh II computer using the software NMR II. A presaturation of the solvent was used for all the 1-D and 2-D ^1H experiments. Four spectra from 280 to 310 K were recorded.

The Selective Inept (INAPT)[25b] recorded with 32 K data points with a selective excitation of the Me and 2-H protons allows us to differentiate carbons. The ^1H detected ^1H,^{13}C HMBC spectrum[33] (PGF-HMBC, pulse gradient field heteronuclear multiple-quantum correlation) was recorded at 300 K with 16 scans, 256 experiments of 1024 data points, a sweep width of 4000 Hz in f_2 and 27507 Hz in f_1. One millisecond half-sinusoid gradients of 28, 28, and -14 G cm^{-1} were used to select for protons attached to carbon and the delay of 80 ms that was optimum for two- or three-bond couplings.

The 2-D J δ selective INEPT[27] using the polarization transfer from ^1H to ^{13}C gave long-range heteronuclear coupling constants ^3J (^{13}C–^1H). The selective excitation of a proton signal allows detection of a single doublet for the corresponding coupled carbon(s). At 500 MHz, selectivity was achieved by a DANTE-type pulse train generated by the decoupler channel. In this study, the ^3J (^{13}C–^1H) coupling constants were measured for the two rotors: the H(2) proton was excited for the H(2)–C(2)–C(3)–C(4) and the H(4) proton for the H(4)–C(4)–C(3)–C(2), but if ambiguity remained as to the assignments of the individual diastereotopic protons, we used their corresponding $^3J'$ (^{13}C–^1H) coupling constants to determine their assignments. This experiment also allows us to analyse the 'A, B, and C' and the 'a, b, and c' rotamer populations. This experiment was recorded at 300 K with 256 scans of 4000 data points, 64 experiments, a spectral width of 220 ppm in f_2 and 62.5 Hz in f_1.

Computer simulations

The conformations of the methylated α-amino acids compounds that were incorporated into the analysis were obtained using the BIOSYM molecular modelling software on a Silicon Graphics workstation.

Initial structures were built using the INSIGHT II builder module, which directly produced coarse 3-D starting structures. To mimic ionization at neutral pH, an sp_3^+ hybridization was assigned to the amine of the main alkyl chain, increasing the molecular electrostatic total charge by +1. To mimic the solvent effect, the relative dielectric constant was set to be distance-dependent in the description of the coulombic interaction, $\varepsilon = R_{ij}$ ($\varepsilon = 5$).[16] A second protocol can be used with explicit solvent molecules incorporated during the run. We constructed solvation boxes containing the glutamate analogue molecule and several water molecules using periodic boundary conditions. A cut-off function of 11 Å was applied for non-bonded interactions. The relative dielectric constant was set to $\varepsilon = 1$ and a box contained 48 (12–12–12) water molecules. The energies obtained are those of 'molecule + 48 H_2O' systems.

Energy minimization and MD simulations were performed with the INSIGHT II Discover module,[34] using the consistent valence force field (CVFF). The first step in the modelling consisted of minimizing the structure previously constructed, to find a local energy minimum on the potential energy hypersurface of the molecule. Calculations were performed according to several algorithms commonly used in molecular mechanics for choosing descent directions, namely steepest descent and conjugate gradient methods.

The second step of the conformational sampling procedure consisted of recording MD trajectories. By solving the equations of motion for a system of atoms, MD has an advantage in that it is not restricted to harmonic motion about a single minimum but allows molecules to cross energy barriers and explore other stable conformations. Molecular conformers were sampled during a 200 ps MD trajectory at 300 K (or 100 ps with 48 water molecules). A time step of 1 fs was used, and the system was equilibrated for 6 ps. A conformation was stored each 1 ps so that 200 conformations (or 100 with 48 water molecules) were recorded by the end of the MD simulation. For a preliminary exploration of the conformational space, after energy minimization and an equilibration period of 6 ps, we performed a 50 ps MD run at 300 K with periodic temperature jumps to 600 K to supply the system with energy (to pass conformational barriers). The 50 ps trajectory is sampled every ps and the remaining structures are then minimized by molecular mechanics and stored. The final conformers found with lowest energies were then further minimized to a gradient less than 0.01 kcal mol^{-1} $Å^2$ to obtain their energies at higher accuracy. For each compound, we have analysed 108 MD simulations. The sampling every picosecond was supposed sufficiently large for a significant displacement of the atoms and sufficiently short

for a correct sampling of the conformational space. For an isolated molecule, the experiment takes about 15–30 min. For experiments in which the molecules are introduced into the solvation boxes, the CPU times are much longer (i.e. 24 or 48 h according to the protocol).

All molecular conformations were compared using the Analysis module of INSIGHT II. Conformational similarities were evaluated by calculating the RMS deviation between heavy atoms for each possible pair of the different structures. The results represent groups of structures whose small RMS deviations (<0.5 Å) suggested that they may belong to the same conformational family. Conformational representatives extracted from each family were compared for each compound, as well as between different ligands, using a superimposition procedure.

Acknowledgement

We thank J. Hart-Davis for skilful assistance with English.

References

1. (a) Watkins, J. C.; Evans, R. H. *Ann. Rev. Pharmacol. Toxicol.* **1981**, *21*, 165; (b) Davies, J.; Evans, R. H.; Francis, A. A.; Jones, D.; Smith, A. S.; Watkins, J. C. *Neurochem. Res.* **1982**, *7*, 1119.

2. Monoghan, D. T.; Bridges, R. J.; Cotman, C. W. *Ann. Rev. Pharmacol. Toxicol.* **1989**, *29*, 365.

3. Bliss, T. V. P.; Collingridge, G. L. *Nature (Lond.)* **1993**, *361*, 31.

4. Choi, D.W. *Neuron* **1988**, *1*, 623.

5. Hollman, M; Heinemann, S. *Ann. Rev. Neurosci.* **1994**, *17*, 31.

6. Nakanishi, S. *Science* **1992**, *258*, 597.

7. Pin, J. P.; Bockaert, J. *Curr. Op. Neurol.* **1995**, *5*, 342.

8. Pin, J. P.; Duvoisin, R. *Neuropharmacology* **1995**, *34*, 1.

9. Conquet, F.; Bashir, Z. I.; Davies, C. H.; Daniel, H.; Ferraguti, F.; Bordi, F.; Franz-Bacon, K.; Reggiani, A.; Matarese, V.; Condé, F.; Colingridge, G. L.; Crépel, F. *Nature (Lond.)* **1994**, *372*, 37.

10. Aiba, A.; Chen, C.; Herrup, K.; Rosenmund, C.; Stevens, C. F.; Tonegawa, S. *Cell* **1994**, *79*, 365.

11. Aiba, A.; Kano, M.; Chen, C.; Stanton, M. E.; Fox, G. D.; Herrupt, K.; Zwingman, A.; Tonegawa, S. *Cell* **1994**, *79*, 377.

12. Kaba, H.; Hayashi, Y.; Higuchi, T.; Nakanishi, S. *Science* **1994**, *265*, 262.

13. O'Hara, P. J.; Sheppard, P. O.; Thøgersen, H.; Venezia, D.; Haldeman, B. A.; McGrane, V.; Houamed, K. M.; Thomsen, C.; Gilbert, T. L.; Mulvihill, E. R. *Neuron* **1993**, *11*, 41.

14. Stern-Bach, Y.; Betler, B.; Hartley, M.; Sheppard, P. O.; O'Hara, P. J.; Heinemann, S. F. *Neuron* **1994**, *13*, 1345.

15. Shimamoto, K.; Ohfune, Y. *J. Med. Chem.* **1996**, 407.

16. (a) Morelle, N.; Gharbi-Benarous, J.; Acher, F.; Valle, G.; Crisma, M.; Toniolo, C.; Azerad, R.; Girault, J. P. *J. Chem. Soc., Perkin Trans. 2* **1993**, 525; (b) Acher, F.; Morelle, N.; Gharbi-Benarous, J.; Valle, G.; Crisma, M.; Toniolo, C.; Azerad, R.; Girault, J. P. *Peptides* **1993**, 581.

17. Larue, V.; Gharbi-Benarous, J.; Acher, F.; Valle, G.; Crisma, M.; Toniolo, C.; Azerad, R.; Girault, J. P. *J. Chem. Soc., Perkin Trans. 2* **1995**, 1111.

18. (a) James, V. A.; Walker, R. J.; Wheal, H. V. *Br. J. Pharmacol.* **1980**, *68*, 711; Johnston, G. A. R.; Curtis, D. R.; Davies, J.; McCulloch, R. M. *Nature (Lond.)* **1974**, *248*, 804; (b) Hall, J. G.; Hicks, T. P.; McLennan, H.; Richardson, T. L.; Wheal, H. V. *J. Physiol.* **1979**, *286*, 29; Wheal, H. V.; Kerkut, G. A. *Comp. Biochem. Physiol.* **1976**, *53C*, 51.

19. (a) Acher, F.; Azerad, R. *Tetrahedron: Asymmetry* **1994**, *5*, 731; (b) Trigalo, F.; Molliex, C.; Champion, B.; Azerad, R. *Tetrahedron Lett.* **1991**, *32*, 3049.

20. (a) Pin, J. P.; Waeber, C.; Prézeau, L.; Bockaert, J.; Heinemann, S. F. *Proc. Natl. Acad. Sci. U.S.A.* **1992**, *89*, 10331; (b) Pin, J. P.; Bockaert, J.; Pittaway, K. M., Sunter, D. C. private communication.

21. Gu, Z. Q.; Hesson, D. P.; Pelletier, J. C.; Maccecchini, M. L. *J. Med. Chem.* **1995**, *38*, 2518.

22. Ouerfelli, O.; Ishida, M.; Shinosaki, H.; Nakanishi, K.; Ohfune, Y. *Synlett* **1993**, 409.

23. Todeschi, N.; Gharbi-Benarous, J.; Girault, J. P. private communication.

24. Ham, N. S. In *Molecular and Quantum Pharmacology*; Bergmann, E.; Pullman, B., Eds.; Dordrecht: Holland, 1974; p 261.

25. (a) Bendall, M. R.; Pegg, D. T. *J. Magn. Reson.* **1983**, *53*, 272; (b) Bax, A. *J. Magn. Reson.* **1984**, *57*, 314; (c) Linand, L. J.; Cordell, G. A. *J. Chem. Soc., Chem. Commun.* **1986**, 377.

26. (a) De Marco, A.; Llinas, M.; Wüthrich, K. *Biopolymers* 1978, *17*, 637; De Marco, A.; Llinas, M.; Wüthrich, K. *Biopolymers* **1978**, *17*, 2727; (b) De Marco, A.; Llinas, M. *Biochemistry* **1979**, *18*, 3846. (c) Roberts, G. C. K.; Jardetzky, O. *Adv. Prot. Chem.* **1970**, *24*, 447; (d) Jardetzky, O.; Roberts, G. C. K. *NMR in Molecular Biology*; Academic: New York, 1981; pp 147–150.

27. Ladam, P.; Gharbi-Benarous, J.; Pioto, M.; Delaforge, M.; Girault, J. P. *Magn. Reson. Chem.* 1994, *32*, 1.

28. (a) Altona, C.; Sundaralingam, M. *J. Am. Chem Soc.* **1973**, 95, 2333; Haasnoot, F. A.; de Leeuw, A. M.; Altona, C. *Tetrahedron* **1980**, 36, 2783; (b) Tvaroska, I.; Hricovini, M.; Petrakova, E. *Carbohydr. Res.* **1989**, *189*, 359.

29. Burt, S. K.; Mackay, D.; Nagler, A. T. In *Computer-Aided Drug Design*; Perun, T.J.; Propst, C. L., Eds.; Marcel Dekker: New York, 1989; p 66.

30. Kollmann, P. *J. Am. Chem. Soc.* **1984**, *106*, 765.

31. (a) Yanagida, M.; Hashimoto, K.; Ishida, M.; Shinozaki, H.; Shirahama, H. *Tetrahedron Lett.* **1989**, *29*, 3799; (b) Hashimoto, M.; Hashimoto, K.; Shirahama, H. *Tetrahedron* **1996**, *6*, 1931.

32. Ortwine, D. F.; Malone, T. C.; Bigge, C. F.; Drummond, J. T.; Humblet, C.; Johnson, G.; Sheppard, P. O. *J. Med. Chem.* **1992**, *35*, 1345.

33. Hurd, R. E.; John, B. K. *J. Magn. Reson.* **1991**, *91*, 648.

34. Dauber-Osguthorpe, P.; Roberts, V. A.; Osguthorpe, D. J.; Wolff, J.; Genest, M.; Hagler, A. T. *Proteins: Struct., Funct., Genet.* **1988**, *4*, 31.

(*Received in U.S.A.* 24 *June* 1996; *accepted* 19 *September* 1996)